J. Fluid Mech. (2013), *vol.* 715, *pp.* 103–133. © Cambridge University Press 2013
doi:10.1017/jfm.2012.502

The oblique parabolic equation model for linear and nonlinear wave shoaling

Yaron Toledo†

ISS, Faculty of Mechanical Engineering, Wuppertal University, Talstrasse 71, 42551 Velbert, Germany

(Received 30 March 2012; revised 5 October 2012; accepted 9 October 2012)

Common simplified models for surface gravity waves result in parabolic-type equations. These equations mostly assume a negligible reflection from the bottom variations but account for both refraction and diffraction effects. A common deficiency of these equations is an inherent assumption of normally incident waves, which cause an increasing error, as the incident waves propagate from an increasing attack angle. In the nonlinear formulation of this type of equation, previous research added the assumption of small crossing angles between interacting waves, which also limits the applicability of these nonlinear models to narrow directional spectra. The current paper presents a parabolic approximation for oblique incident waves that overcomes these limitations. This is done by introducing a perturbation solution for the wave's phase function, which in its lowest order corresponds to oblique incident waves on a bottom with no lateral changes. The resulting curved wave ray structure replaces the simplified straight one used in the derivation process of various former models. In the nonlinear model, the nonlinear interactions are calculated between the frequency modes while taking into account the different propagating directions. Numerical results of the oblique parabolic equation show great advantages compared to other formulations that use a straight wave ray structure and the small crossing angle assumption. The nonlinear model was used to investigate the nonlinear shoaling of two similar monochromatic waves approaching from different angles. This fundamental nonlinear interaction problem shows that there is an energy transfer to waves of the primary harmonic that approach at larger attack angles than the two incident waves. This is counter-intuitive. Unlike in the case of linear wave shoaling, where the waves reduce their attack angle in the refraction process, in the nonlinear shoaling process the attack angle can increase. Fundamental numerical simulations of the linear and nonlinear oblique parabolic models are shown to be in excellent agreement with the initial mild-slope equations. This confirms the benefits of applying these models to various shoaling scenarios for both linear and nonlinear waves.

Key words: surface gravity waves, waves/free-surface flows

1. Introduction

The flow of surface water waves is a time-varying three-dimensional problem. In various scenarios, it is plausible to assume that the flow is governed by the Laplace equation together with free-surface and impermeable bottom boundary

† Email address for correspondence: yaron.toledo@gmail.com

https://doi.org/10.1017/jfm.2012.502 Published online by Cambridge University Press

conditions. The three-dimensional problem is complicated to model, and its solution requires significant computational effort. Therefore, in many applications, the vertical dimension is reduced in order to simplify the model. A commonly employed approach for this reduction yields the frequency domain mild-slope-type equations, which apply to linear time-harmonic problems. The origin of this discipline is the mild-slope equation based on the works of Biesel (1952), Eckart (1952), Svendsen (1967) and Berkhoff (1972) for time-harmonic waves. The mild-slope equation and other mild-slope-type models achieve this reduction by applying a predefined vertical profile for the flow followed by integration over the depth. Many works have continued the derivation of the mild-slope equation (e.g. Massel 1993; Chamberlain & Porter 1995; Porter & Staziker 1995; Agnon 1999; Porter 2003; Kim & Bai 2004; Hsu *et al.* 2006; Porter & Porter 2006; Toledo & Agnon 2010*a*,*b*).

The mild-slope equations can be simplified further. By applying a parabolic approximation, mild-slope equations reduce from elliptic equations to parabolic ones while still accounting for refraction and diffraction effects. This approach, which was formerly applied to the Helmholtz equation in the field of underwater acoustic waves (see e.g. McDaniel 1975), was adapted to the field of water waves by its application to mild-slope-type equations while neglecting wave reflection (see e.g. Liu & Mei 1976; Radder 1979). Nonetheless, there are models that can account for this phenomenon using two coupled parabolic equations (see Liu & Tsay 1983; Dingemans 1997, § 3.6.2). A review of parabolic equations for surface gravity waves is given by Martin, Dalrymple & Kirby (1997).

The wave propagation problem in the field of underwater acoustics differs from that in surface gravity waves in several respects. The two-dimensional problem in acoustics relates to a thin-layer one, as the water depth is much smaller than the propagation distance. The sound waves are normally transmitted in narrow horizontal angles and, even if they are not, the sound energy propagating in large angles will mostly be dissipated, since it loses energy due to impacts with the sea surface and the sea bottom. In any case, the area of interest for these models is the far field. Hence, the basic assumption of normally incident waves incorporated in these derivations is suitable. There are methods for extending the accuracy of these equations to wider angles, for instance the minimax approach, which reduces the error by an averaging process over a predefined range of wave angles (see Greene 1984).

In the field of surface gravity waves, however, the horizontal domain is not suited to a thin-layer assumption. In addition, frequently the waves approach the beach from large oblique incident angles, so that the normal incidence wave assumption (or a straight wave ray assumption) is unsuitable. In order to increase accuracy, high-order equations have been used (see Kirby 1986*a*): the minimax approach was applied (see Kirby 1986*b*), and an averaging technique was imposed (see Lozano & Liu 1980). Each method has its own advantages and disadvantages. Higher-order methods have improved accuracy but with the cost of a more demanding numerical solution. The minimax approach reduces the general error, but still produces errors that increase even for the normally incident case as the attack angle increases.

The averaging technique uses an averaged wavenumber that corresponds to a bottom profile that is averaged over the lateral span of a calculation. It has shown good results but may create some inconsistencies. For example, consider the wave propagation problem over a flat bottom with an underwater mount. The averaged bottom profile is dependent on the size of the lateral length of the domain. Nevertheless, increasing this size in the case of a continuous beach should not affect the actual physical problem, but it does affect the averaged wavenumber and thus the parabolic model

https://doi.org/10.1017/jfm.2012.502 Published online by Cambridge University Press

itself. Another example is a constant mild lateral linear slope. The average is a good approximation near the centreline of the calculation domain, but for a large lateral span, the farther we get from the centreline the greater the difference between the averaged depth and the local one.

Another approach for improving parabolic approximations with negligible reflection takes into account a curved ray structure. Liu & Mei (1976) have derived a model using curved ray paths while assuming no depth changes in the lateral direction. The resulting model has a general formulation, which requires the solution also along the vertical axis in order to enable solution of the diffraction problem near a shadow boundary. Tsay & Liu (1982) combined the ray-theory approach with the parabolic one by finding the wave rays' amplitude and directions using a simple geometric optic solution and then correcting it by solving a parabolic equation for the diffraction function (see also Tsay, Ebersole & Liu 1989 for a boundary-fitted curvilinear coordinate system parabolic model). Dalrymple & Kirby (1988) have extended the applicability of parabolic equations using a Fourier transformation in the lateral direction, solving the resulting ordinary differential equations and applying the inverse transform (see also Dalrymple & Kirby 1992). Isobe (1987) derived a parabolic equation along a wave ray where the ray's direction was calculated *a priori* using Snell's law and applied this model to calculation of random waves. For the same purpose, Mase (2001) used Radder's parabolic equation to introduce diffraction effects into a wave action equation formulation. A more simplified approach was presented by Liu & Tsay (1985). There, an average bottom approach was used while taking into account an oblique incident wave. In this case, the wave ray solution could be calculated using a simple one-dimensional integration, as no lateral changes are taken into account for the averaged profile. A parabolic equation was then formulated along the curved ray path.

As waves shoal, and their steepness increases, quadratic nonlinear terms may no longer be discarded. A nonlinear mild-slope equation model was derived by Kaihatu & Kirby (1995) consisting of quadratic nonlinear coupling terms between wave modes; see Toledo & Agnon (2009) for a quadratic nonlinear derivation extending the linear streamfunction formulation of Kim & Bai (2004). Then a parabolic approximation for forward-propagating waves was applied, using normal incidence wave ray structure assumptions, a small crossing angle between interacting waves, and the averaging technique (laterally averaged depth profile). Janssen, Herbers & Battjes (2006) have also derived a related model using the same assumptions, but by decomposing the wave solution to a laterally averaged bottom profile and its weaker two-dimensional correction. Kaihatu (2001) has improved the linear part of Kaihatu & Kirby's model to account for wide-angle waves using the model of Kirby (1986*a*). Nevertheless, this model's nonlinear part retained the assumption of small crossing angles between interacting waves, which reduces the ability of this model to accurately account for the nonlinear interactions in the case of wide-angle waves. Janssen, Herbers & Battjes (2008) extended the Fourier approach (in the lateral direction) of Dalrymple & Kirby (1988) to quadratic nonlinearity. This model, which was also written in stochastic form, used a sum of wave directions in each wave harmonic as in the hyperbolic formulations of Agnon *et al.* (1993) and Herbers & Burton (1997) for wave shoaling over a bottom with no lateral changes. Nevertheless, even while taking into account wave directionality, the formulation of Janssen *et al.* (2008) still assumed small crossing angles between the interacting waves.

The main limitation to most of the above parabolic approximations is that they are based on the assumption of a straight wave ray structure parallel to a predefined

https://doi.org/10.1017/jfm.2012.502 Published online by Cambridge University Press

direction. This results in inaccurate solutions to the most fundamental problem of oblique incident waves propagating over a beach with no lateral bottom changes (parallel depth contours), which follow curved ray paths. The error of these solutions grows as the attack angle increases. It also relates to the main limitation in the derivation of the quadratic nonlinear terms of these equations, as it imposes a small crossing angle approximation. The first goal of this paper is to provide a linear parabolic equation such as that of Radder (1979), which does not hold the above limiting approximation for oblique incident waves. The second goal is to provide an alternative for using the averaged bottom approach and allow for lateral changes in the approximated wave ray structure used for the parabolic approximation. This will be done by deriving a perturbation solution for the wavenumber vector and its phase in the case of mild lateral bottom changes. The third goal of this work is to extend the oblique parabolic model to account for quadratic nonlinear interactions without the limiting assumption of small crossing angles between the interacting waves.

The paper is constructed as follows. In § 2 the nonlinear mild-slope equation is presented and its linear part is reduced to the Helmholtz equation. In § 3 a linear parabolic equation is constructed without the assumption of a normal incidence wave ray structure. The perturbation solution for the wavenumber vector and the phase function is derived in § 4, and the parabolic equation is extended to account for quadratic nonlinear interactions in § 5. Nonlinear relations between the velocity potentials and the wave elevations are derived in § 6. Numerical calculations are presented in § 7, and the work is summarized and discussed in § 8.

2. The nonlinear mild-slope equation model

The quadratic nonlinear mild-slope equation (see Kaihatu & Kirby 1995, equation 22) is given by

$$\begin{aligned}
&\nabla\cdot\left[\left(CC_g\right)_n\nabla\phi_n\right]+\left[k_n^2\left(CC_g\right)_n+gR_n\right]\phi_n\\
&\quad=-\frac{\mathrm{i}}{4}\sum_{l=1}^{N-1}\left\{2\omega_n\nabla\phi_l\cdot\nabla\phi_{n-l}+\omega_l\phi_l\nabla^2\phi_{n-l}+\omega_{n-l}\phi_{n-l}\nabla^2\phi_l\right.\\
&\qquad\left.+\frac{\omega_l\omega_{n-l}\omega_n}{g^2}\left(\omega_l^2+\omega_l\omega_{n-l}+\omega_{n-l}^2\right)\phi_l\phi_{n-l}\right\}\\
&\qquad-\frac{\mathrm{i}}{2}\sum_{l=1}^{N-n}\left\{2\omega_n\nabla\phi_l^*\cdot\nabla\phi_{n+l}+\omega_{n+l}\phi_{n+l}\nabla^2\phi_l^*-\omega_l\phi_l^*\nabla^2\phi_{n+l}\right.\\
&\qquad\left.-\frac{\omega_l\omega_{n+l}\omega_n}{g^2}\left(\omega_l^2-\omega_l\omega_{n+l}+\omega_{n+l}^2\right)\phi_l^*\phi_{n+l}\right\}\equiv NL_n,
\end{aligned}\tag{2.1}$$

with higher-order bottom terms

$$R_n=r_{1,n}\nabla^2h+r_{2,n}\left|\nabla h\right|^2,\tag{2.2}$$

$$r_{1,n}=\frac{\operatorname{sech}^2k_nh}{4\left(2k_nh+\sinh 2k_nh\right)}\left(\sinh 2k_nh-2k_nh\cosh 2k_nh\right),\tag{2.3}$$

$$\begin{aligned}
r_{2,n}=&\frac{k_n\operatorname{sech}^2k_nh}{12(2k_nh+\sinh 2k_nh)^3}[(2k_nh)^4+4(2k_nh)^3-9\sinh 2k_nh\sinh 4k_nh\\
&+6k_nh(2k_nh+2\sinh 2k_nh)(\cosh^2 2k_nh-2\cosh 2k_nh+3)],
\end{aligned}\tag{2.4}$$

https://doi.org/10.1017/jfm.2012.502 Published online by Cambridge University Press

which were added to the original formulation. In accordance with mild-slope-type models, the velocity potential Φ was assumed to be constructed of a superposition of solutions with a known vertical profile

$$\Phi\,(x, y, z, t) = \frac{1}{2}\sum_{n=1}^{N} f_n\,(k_n, h, z)\left(\phi_n(x, y)\mathrm{e}^{-\mathrm{i}\omega_n t} + \phi_n^*(x, y)\mathrm{e}^{\mathrm{i}\omega_n t}\right), \tag{2.5}$$

where

$$f_n = \frac{\cosh k_n\,(z + h)}{\cosh k_n h}, \tag{2.6}$$

$$\omega_n^2 = g k_n \tanh k_n h. \tag{2.7}$$

Here, the vertical coordinate z of the Cartesian coordinate system $Oxyz$ directs upward with the Oxy-plane located on the horizontal still-water surface, and $*$ represents the complex conjugate. The components constructing (2.1)–(2.7) are defined as follows: $\Phi(x, y, z, t)$ is the wave velocity potential, $h(x, y)$ is the bottom profile, ∇ is the horizontal gradient operator, and C_n and $C_{g,n}$ are the modal phase and group velocities respectively. The modal wavenumber k_n is related to the modal angular frequency ω_n through the dispersion relation for linear surface gravity waves (2.7). Equations (2.2)–(2.4) describe the higher-order bottom derivative components given by Massel (1993) and Chamberlain & Porter (1995), and the phase and group velocities are given by

$$C_n = \frac{\omega_n}{k_n}, \quad C_{g,n} = \frac{1}{2}\frac{\omega_n}{k_n}\left(1 + \frac{2k_n h}{\sinh\,(2k_n h)}\right). \tag{2.8}$$

The nonlinear part of (2.1) can be simplified by using its linear part and neglecting terms of $O((ka)^2\,|\partial h/\partial x|, (ka)^2\,|\partial h/\partial y|, (ka)^2\,|\nabla^2 h|, (ka)^2\,|\nabla h|^2)$ to yield

$$\begin{aligned} NL_n = {} & \frac{\mathrm{i}}{4}\sum_{l=1}^{N-1}\left\{-2\omega_n \nabla\phi_l \cdot \nabla\phi_{n-l}\right. \\ & \left. + \left[\omega_l k_{n-l}^2 + \omega_{n-l}k_l^2 - \frac{\omega_l\omega_{n-l}\omega_n}{g^2}\left(\omega_l^2 + \omega_l\omega_{n-l} + \omega_{n-l}^2\right)\right]\phi_l\phi_{n-l}\right\} \\ & - \frac{\mathrm{i}}{2}\sum_{l=1}^{N-n}\left\{2\omega_n \nabla\phi_l^* \cdot \nabla\phi_{n+l}\right. \\ & \left. + \left[\omega_l k_{n+l}^2 - \omega_{n+l}k_l^2 - \frac{\omega_l\omega_{n+l}\omega_n}{g^2}\left(\omega_l^2 - \omega_l\omega_{n+l} + \omega_{n+l}^2\right)\right]\phi_l^*\phi_{n+l}\right\}. \end{aligned} \tag{2.9}$$

In the ordering procedure, the wave slope ka was taken as the maximum value over the N modal wave slopes $k_n a_n$.

By applying the Liouville transform (see e.g. Radder 1979; Dingemans 1997; Hsu & Wen 2001, § 3.7.3), one can write the linear part of (2.1) as a Helmholtz equation. This is done by introducing the scaling factor

$$\hat{\phi}_n = \phi_n\,(CC_g)_n^{1/2}, \tag{2.10}$$

which, after application to the linear part, turns (2.1) into

$$\nabla^2\hat{\phi}_n + k_{c,n}^2\hat{\phi}_n = \left(CC_g\right)_n^{-1/2} NL_n. \tag{2.11}$$

https://doi.org/10.1017/jfm.2012.502 Published online by Cambridge University Press

The effective wavenumber $k_{c,n}$ is defined by

$$k_{c,n}^2 = k_n^2 - \left(CC_g\right)_n^{-1/2} \nabla^2 \left(CC_g\right)_n^{1/2} + \left(CC_g\right)_n^{-1} gR_n. \tag{2.12}$$

For the case of a small bottom slope that induces negligible reflection, terms of $O(|\nabla h|^2)$ may be neglected, as they should fulfil the following criterion:

$$\left(\frac{\nabla h}{kh}\right)^2 \ll 1 \tag{2.13}$$

(see discussion in Dingemans 1997, § 3.6.2). In this case, the effective wavenumber can be further simplified to

$$k_{c,n}^2 = k_n^2 - \left[\frac{1}{2}\left(CC_g\right)_n^{-1} \frac{\partial \left(CC_g\right)_n}{\partial h} - \left(CC_g\right)_n^{-1} gr_{1,n}\right] \nabla^2 h = k_n^2 + \left(CC_g\right)_n^{-1} \bar{r}_n \nabla^2 h. \tag{2.14}$$

The contribution of the bottom curvature $O(\nabla^2 h)$ in the definition of $k_{c,n}$ can also be neglected (i.e. setting $k_{c,n} = k_n$) when

$$\left|\frac{\nabla^2 h}{k^2 h}\right| \ll 1 \tag{2.15}$$

(see the same discussion in Dingemans 1997). The criterion given in (2.15) is mostly fulfilled for wave scenarios with negligible reflection due to the mildness of the bottom slope. However, it may have an effect when there are corners in the bottom profile that cause spikes (Dirac δ functions) in the bottom curvature function. This case should be handled separately, and remains beyond the scope of this paper.

3. Derivation of the parabolic approximation of the linear equation for forward-propagating waves

In order to apply a parabolic approximation to (2.11), the splitting matrix method will be used as in Radder (1979). The first step in this method separates the wave field into a transmitted field $\hat{\phi}_n^+$ and a reflected one $\hat{\phi}_n^-$,

$$\hat{\phi}_n = \hat{\phi}_n^+ + \hat{\phi}_n^-. \tag{3.1}$$

A splitting matrix is used in order to relate the transmitted and reflected components to the wave field and its shore-directed x-derivative:

$$\begin{pmatrix} \hat{\phi}_n^+ \\ \hat{\phi}_n^- \end{pmatrix} = \boldsymbol{T}_n \begin{pmatrix} \hat{\phi}_n \\ \dfrac{\partial \hat{\phi}_n}{\partial x} \end{pmatrix} \equiv \begin{pmatrix} \alpha_n & \beta_n \\ \gamma_n & \delta_n \end{pmatrix} \begin{pmatrix} \hat{\phi}_n \\ \dfrac{\partial \hat{\phi}_n}{\partial x} \end{pmatrix}. \tag{3.2}$$

The arbitrary matrix $\boldsymbol{T}_n$ is limited by some general physical criteria that yield the parabolic model in a natural way. The first set of two restrictions result from the definition given in (3.1), which for the linear part are given by

$$\alpha_n + \gamma_n = 1, \quad \beta_n + \delta_n = 0. \tag{3.3}$$

https://doi.org/10.1017/jfm.2012.502 Published online by Cambridge University Press

Taking the x-derivative of equation set (3.2) and applying (3.1) and (2.11) yields

$$\frac{\partial \hat{\phi}_n^+}{\partial x} - \left(-k_{c,n}^2\beta_n + \frac{\alpha_n\gamma_n}{\beta_n} + \frac{\partial \alpha_n}{\partial x} + \frac{\gamma_n}{\beta_n}\frac{\partial \beta_n}{\partial x} - \beta_n\frac{\partial^2}{\partial y^2}\right)\hat{\phi}_n^+ = \left(-k_{c,n}^2\beta_n - \frac{\alpha_n^2}{\beta_n} + \frac{\partial \alpha_n}{\partial x} - \frac{\alpha_n}{\beta_n}\frac{\partial \beta_n}{\partial x} - \beta_n\frac{\partial^2}{\partial y^2}\right)\hat{\phi}_n^-, \tag{3.4}$$

$$\frac{\partial \hat{\phi}_n^-}{\partial x} - \left(k_{c,n}^2\beta_n - \frac{\alpha_n\gamma_n}{\beta_n} + \frac{\partial \gamma_n}{\partial x} + \frac{\alpha_n}{\beta_n}\frac{\partial \beta_n}{\partial x} + \beta_n\frac{\partial^2}{\partial y^2}\right)\hat{\phi}_n^- = \left(k_{c,n}^2\beta_n + \frac{\gamma_n^2}{\beta_n} + \frac{\partial \gamma_n}{\partial x} - \frac{\gamma_n}{\beta_n}\frac{\partial \beta_n}{\partial x} + \beta_n\frac{\partial^2}{\partial y^2}\right)\hat{\phi}_n^+. \tag{3.5}$$

Up to this point the derivation has followed closely the one of Radder (1979), with (3.4) and (3.5) differing only by the use of $k_{c,n}^2$ instead of k_n^2.

For a constant depth or the case of deep water, (3.4) and (3.5) should yield the solutions

$$\hat{\phi}_n^+ \sim \mathrm{e}^{\mathrm{i}k_{01,n}x + \mathrm{i}k_{02,n}y}, \quad \hat{\phi}_n^- \sim \mathrm{e}^{-\mathrm{i}k_{01,n}x + \mathrm{i}k_{02,n}y}, \tag{3.6}$$

with

$$\boldsymbol{k}_{0,n} = \left(k_{01,n}, k_{02,n}\right)^{\mathrm{T}}, \quad |\boldsymbol{k}_{0,n}|^2 = k_{0,n}^2, \tag{3.7}$$

where the subscript zero represents the quantities in deep water. Note that (3.6) defines waves in a general propagation direction. Here lies a major difference between the current derivation and various other previous studies, where the constant wavenumber solution was assumed to be of the form $\mathrm{e}^{\pm \mathrm{i}k_{0,n}x}$. This former assumption corresponds only to an incident/reflected wave propagating in a straight wave ray structure, without the possibility of accounting for the curved ray structures that are common in oblique incident wave propagation.

Letting the simple solutions (3.6) satisfy (3.4) and (3.5) yields a second set of restrictions:

$$k_{01,n}^2\beta_n + \alpha_n^2/\beta_n = 0, \quad k_{01,n}^2\beta_n + \gamma_n^2/\beta_n = 0, \tag{3.8}$$

$$\mathrm{i}k_{01,n,m} = -k_{01,n}^2\beta_n + \frac{\alpha_n\gamma_n}{\beta_n}. \tag{3.9}$$

Solving (3.3) and (3.8)–(3.9) for the splitting matrix components results in

$$\boldsymbol{T}_{0,n} = \frac{1}{2}\begin{pmatrix} 1 & -\mathrm{i}/k_{01,n} \\ 1 & \mathrm{i}/k_{01,n} \end{pmatrix}. \tag{3.10}$$

Hence, an educated guess for the solution of the splitting matrix for the case of a varying bottom can be given by

$$\boldsymbol{T}_n = \frac{1}{2}\begin{pmatrix} 1 & -\mathrm{i}/k_{1,n} \\ 1 & \mathrm{i}/k_{1,n} \end{pmatrix}, \tag{3.11}$$

with

$$\boldsymbol{k}_n = \left(k_{1,n}, k_{2,n}\right)^{\mathrm{T}}, \quad |\boldsymbol{k}_n|^2 = k_n^2. \tag{3.12}$$

In order to confirm this educated guess, let us inspect the case of linear wave propagation for mild slopes, where wave reflection can be neglected. In this case, $\hat{\phi}_n^+$

https://doi.org/10.1017/jfm.2012.502 Published online by Cambridge University Press

and $\hat{\phi}_n^-$ can be decoupled and should each satisfy the Helmholtz equation (i.e. the linear part of (2.11)) without affecting each other. Substituting the splitting matrix (3.11) for the x-derivative of (3.4) while neglecting the reflected waves $\hat{\phi}_n^-$ and terms of $O((\partial h/\partial x)^2, (\partial h/\partial y)^2, |(\partial h/\partial x)(\partial h/\partial y)|)$ reconstructs the Helmholtz equation for $\hat{\phi}_n^+$ in the case of small changes in the lateral direction. This implies the ordering hierarchy $\delta \ll \mu \ll 1$, where $|\partial h/\partial x| = O(\mu)$ and $|\partial h/\partial y| = O(\delta)$.

By neglecting $\hat{\phi}_n^+$, the x-derivative of (3.5) yields the Helmholtz equation for $\hat{\phi}_n^-$, which can also be solved by the trivial solution $\phi_n^- = 0$. This trivial solution relates to the case where waves are entering the calculation domain only from the direction of the negative x-axis and the slopes are mild enough to cause no significant reflection. Note that the Helmholtz equation is satisfied only by neglecting terms of $O((\partial h/\partial x)^2, (\partial h/\partial y)^2, |(\partial h/\partial x)(\partial h/\partial y)|)$ (i.e. with $k_{c,n}$ defined by (2.14)).

Substituting the splitting matrix (3.11) for (3.4) with an assumption of negligible wave reflection and no wave entry from the positive x-axis $\left(\phi^- \backsimeq 0\right)$ yields

$$\frac{\partial \hat{\phi}_n^+}{\partial x} = \left(\frac{\mathrm{i}\left(k_{c,n}^2 + k_{1,n}^2\right)}{2k_{1,n}} - \frac{1}{2k_{1,n}} \frac{\partial k_{1,n}}{\partial x} + \frac{\mathrm{i}}{2k_{1,n}} \frac{\partial^2}{\partial y^2} \right) \hat{\phi}_n^+. \tag{3.13}$$

At this point the wavenumber component $k_{1,n}$ in (3.13) is still unknown. This gap will be filled in § 4 via a perturbation approach, where δ will be used as a small parameter.

Equation (3.13) can be written in terms of the velocity potential using (2.10) and the assumption of negligible wave reflection

$$\hat{\phi}_n^+ = \left(CC_g\right)_n^{1/2} \phi_n^+ \backsimeq \left(CC_g\right)_n^{1/2} \phi_n. \tag{3.14}$$

This results in the linear oblique parabolic equation (OPE):

$$2\mathrm{i}k_{1,n}\left(CC_g\right)_n \frac{\partial \phi_n}{\partial x} + \left[\left(k_{c,n}^2 + k_{1,n}^2\right)\left(CC_g\right)_n + \mathrm{i}\frac{\partial}{\partial x}\left(k_{1,n}\left(CC_g\right)_n\right) \right] \phi_n + \frac{\partial}{\partial y}\left(\left(CC_g\right)_n \frac{\partial \phi_n}{\partial y} \right) = 0. \tag{3.15}$$

Equation (3.15) is the first main result of this paper. It defines a parabolic equation model with inherent oblique wave propagation characteristics. In the case of incident waves along the x-axis (i.e. $k_{2,n} = 0$) and after neglecting terms of the bottom curvature $O(\nabla^2 h)$, (3.15) reduces to the parabolic equation of Radder (1979). A discussion on the behaviour of the OPE in the case of oblique incident waves will be given in §§ 4 and 8.

4. A perturbation solution for the wavenumber vector and phase function of oblique incident waves

Liu & Tsay (1985) presented a semi-analytical approach for solving oblique incident waves using a parabolic equation model. They assumed a laterally averaged bottom profile (i.e. throwing out lateral changes in the bottom profile as well as lateral derivatives) and solved the amplitudes and directions of a wave ray propagation using a simple one-dimensional integration. Then they corrected the result by solving a parabolic equation for the diffraction function. The aim of this section is to derive semi-analytical solutions for the wavenumber vectors and phase functions in the case of mild lateral bottom changes. This can be regarded as an extended alternative to the approach of Liu & Tsay (1985). The zeroth order of the present perturbation solution

https://doi.org/10.1017/jfm.2012.502 Published online by Cambridge University Press

resembles the semi-analytical solution of Liu & Tsay (1985) but uses the local depth rather than a laterally averaged depth (i.e. keeping some of the effects of the lateral bottom changes) with lateral derivatives being pushed to higher order. The higher-order extensions are dependent on the bottom slope in the lateral direction, which were discarded in the average bottom profile approach.

As a first step in writing the perturbation solution of the wavenumber vectors and phase functions in the case of mild lateral bottom changes, let us write ϕ_n^+ in form of a travelling wave,

$$\phi_n^+ = B_n(x, y)\mathrm{e}^{\mathrm{i}S_n(x,y)}, \tag{4.1}$$

and inspect the wavenumber and phase fields for waves propagating over a general bottom. The phase function S_n of the oscillating flow and the corresponding wavenumber vector $\boldsymbol{k}_n$ are related as follows:

$$\boldsymbol{\nabla} S_n \equiv \boldsymbol{k}_n \equiv \left(k_{1,n}, k_{2,n}\right)^{\mathrm{T}}, \quad k_n \equiv |\boldsymbol{k}_n|. \tag{4.2}$$

Hence, it is easy to construct the relation

$$0 \equiv \boldsymbol{\nabla} \times \boldsymbol{\nabla} S_n = \boldsymbol{\nabla} \times \boldsymbol{k}_n = \frac{\partial k_{1,n}}{\partial y} - \frac{\partial k_{2,n}}{\partial x}, \tag{4.3}$$

which is sometimes referred to as the irrotationality (or the curl) of the wavenumber (see e.g. Young 1999, § 4.2.1). Another equation relating the wavenumber components can be constructed using the Pythagoras theorem, which in the case of forward-propagating waves (in the positive x-direction) takes the form

$$k_{1,n} = \sqrt{k_n^2 - k_{2,n}^2}. \tag{4.4}$$

The corresponding phase function relates to $k_{1,n}$ in the following manner:

$$\frac{\partial S_n}{\partial x} = k_{1,n}, \quad S_n = \int_{x_0}^{x} k_{1,n}(\xi, y)\,\mathrm{d}\xi + \Gamma(y). \tag{4.5}$$

Equations (4.3) and (4.4) govern the wavenumber vector field, but unfortunately they consist of a partial differential equation and a nonlinear algebraic relation. It is possible to decouple this system to a single nonlinear partial differential equation for $k_{2,n}$ and an algebraic definition for $k_{1,n}$. This can be done by substituting (4.4) for (4.3), but it still leaves us with a nonlinear partial differential equation.

In the case of mild lateral bottom changes $|\partial h/\partial y| = O(\delta)$, several helpful assumptions can be made. By inspecting (4.3) one can deduce that the wavenumber component $k_{2,n}$ changes in the x-direction in the same order as $k_{1,n}$ in the y-direction. Taking this into account, the scaling of the wavenumber components can be defined as follows:

$$k_n = k_n\left(\mu x, \delta y\right), \quad k_{1,n} = k_{1,n}\left(\mu x, \delta y\right), \tag{4.6}$$

$$k_{2,n} - k_{02,n} = O(\delta), \quad k_{2,n} = k_{2,n}\left(\delta x, \delta y\right), \tag{4.7}$$

where $k_{02,n}$ is the (constant) deep-water wavenumber in the y-direction, and $\delta \ll \mu \ll 1$. Note that the changes in the lateral direction were taken to be smaller than in the main propagation direction only within the definition of the wavenumber and not in the behaviour of the velocity potential, which still retains second-order derivatives in the lateral direction. This is actually an inherent assumption in other models that use a laterally averaged bottom profile (such as e.g. Lozano & Liu 1980), which yields a

https://doi.org/10.1017/jfm.2012.502 Published online by Cambridge University Press

laterally averaged wavenumber. Clearly, a laterally averaged wavenumber is a plausible quantity only when the lateral bottom changes are small.

The Taylor series of (4.4) centred at $k_{02,n}$ is given by

$$k_{1,n} = \sqrt{k_n^2 - k_{02,n}^2} - \frac{k_{02,n}}{\sqrt{k_n^2 - k_{02,n}^2}}\delta\left(k_{2,n} - k_{02,n}\right) - \frac{k_n^2}{2\left(k_n^2 - k_{02,n}^2\right)^{3/2}}\delta^2\left(k_{2,n} - k_{02,n}\right)^2 + O(\delta^3). \tag{4.8}$$

Substituting (4.8) for (4.3) provides a truncated differential equation for k_2:

$$\frac{k_n}{\sqrt{k_n^2 - k_{02,n}^2}}\frac{\partial k_n}{\partial y}\delta - \frac{\partial k_{2,n}}{\partial x}\delta + \frac{k_{02,n}}{\left(k_n^2 - k_{02,n}^2\right)^{3/2}} \times \left[k_n\left(k_{2,n} - k_{02,n}\right)\frac{\partial k_n}{\partial y} + \left(k_n^2 - k_{02,n}^2\right)\frac{\partial k_{2,n}}{\partial y}\right]\delta^2 = O(\delta^3). \tag{4.9}$$

Equation (4.9) is a partial differential equation for k_2, but as its derivatives for each direction are of different orders, they can easily be separated into two hierarchical ordinary differential equations. In order to do so, a perturbation expansion will be applied in the following manner:

$$k_{2,n} = k_{02,n} + \delta\kappa_{1,n} + \delta^2\kappa_{2,n} + \cdots. \tag{4.10}$$

Substituting (4.10) for (4.9) and separating for different orders of δ yields

$$O(\delta) \quad \frac{\partial \kappa_{1,n}}{\partial x} = \frac{k_n}{\sqrt{k_n^2 - k_{02,n}^2}}\frac{\partial k_n}{\partial y}, \tag{4.11}$$

$$O(\delta^2) \quad \frac{\partial \kappa_{2,n}}{\partial x} = \frac{k_{02,n}}{2\left(k_n^2 - k_{02,n}^2\right)^{3/2}}\left[k_n\left(\kappa_{1,n} - k_{02,n}\right)\frac{\partial k}{\partial y} + \left(k_n^2 - k_{02,n}^2\right)\frac{\partial \kappa_{1,n}}{\partial y}\right]. \tag{4.12}$$

The solutions of (4.11) and (4.12) are given by

$$\kappa_{1,n} = \int_{x_0}^{x} \frac{k_n}{\sqrt{k_n^2 - k_{02,n}^2}}\frac{\partial k_n}{\partial y}\,\mathrm{d}\xi, \tag{4.13}$$

$$\kappa_{2,n} = \int_{x_0}^{x} \frac{k_{02,n}}{2\left(k_n^2 - k_{02,n}^2\right)^{3/2}}\left[k\left(\kappa_{1,n} - k_{02,n}\right)\frac{\partial k_n}{\partial y} + \left(k_n^2 - k_{02,n}^2\right)\frac{\partial \kappa_{1,n}}{\partial y}\right]\mathrm{d}\xi, \tag{4.14}$$

which leads to the reconstruction of $k_{2,n}$:

$$k_{2,n} = k_{02,n} + \delta^2\int_{x_0}^{x}\mathrm{d}\xi\,\frac{k_{02,n}}{2\left(k_n^2 - k_{02,n}^2\right)^{3/2}}\left[k_n\left(\int_{x_0}^{\xi}\frac{k_n}{\sqrt{k_n^2 - k_{02,n}^2}}\frac{\partial k_n}{\partial y}\,\mathrm{d}\zeta - k_{02,n}\right)\frac{\partial k_n}{\partial y} + \left(k_n^2 - k_{02,n}^2\right)\frac{\partial}{\partial y}\int_{x_0}^{\xi}\frac{k_n}{\sqrt{k_n^2 - k_{02,n}^2}}\frac{\partial k_n}{\partial y}\,\mathrm{d}\zeta\right] + \delta\int_{x_0}^{x}\frac{k_n}{\sqrt{k_n^2 - k_{02,n}^2}}\frac{\partial k_n}{\partial y}\,\mathrm{d}\xi + O(\delta^3), \tag{4.15}$$

https://doi.org/10.1017/jfm.2012.502 Published online by Cambridge University Press

where the dummy variables ξ and ζ relate to integration in the x-direction. The solution for $k_{1,n}$ can now be found by substituting (4.15) for (4.8),

$$k_{1,n} = \sqrt{k_n^2 - k_{02,n}^2} - \frac{k_n}{\sqrt{k_n^2 - k_{02,n}^2}}\delta^2 \int_{x_0}^{x} \frac{k_n}{\sqrt{k_n^2 - k_{02,n}^2}} \frac{\partial k_n}{\partial y}\,\mathrm{d}\xi + O(\delta^3), \tag{4.16}$$

which results in solving the entire wavenumber field. The phase function S_n, whose derivatives in the x and y directions result in $k_{1,n}$ and $k_{2,n}$ respectively (see (4.2)), is given by

$$\begin{aligned} S_n = {} & k_{02,n} y + S_{0,n} + \delta \int_{x_0}^{x} \sqrt{k_n^2 - k_{02,n}^2}\,\mathrm{d}\xi \\ & - \delta^2 \int_{x_0}^{x} \frac{k_{02,n}}{\sqrt{k_n^2 - k_{02,n}^2}} \int_{x_0}^{\xi} \frac{k_n}{\sqrt{k_n^2 - k_{02,n}^2}} \frac{\partial k_n}{\partial y}\,\mathrm{d}\zeta\,\mathrm{d}\xi + O(\delta^3), \end{aligned} \tag{4.17}$$

with the constant $S_{0,n}$ representing the initial phase. Equations (4.15)–(4.17) represent the second main finding of this paper. They consist of the perturbation solution for the wavenumber vector and the phase function for a bathymetry with mild lateral changes.

Let us inspect (4.15)–(4.17) further. An assumption of no changes in the lateral direction degenerates these equations to the classical case of a quasi-two-dimensional formulation for oblique incident waves propagating over a bottom with no lateral changes ($k_{2,n} = k_{02,n} = \text{const.}$). For the case of mild changes in the lateral direction, even a lower order of the perturbation solution (i.e. up to $O(\delta)$) gives an extension. This simple case can be written as

$$k_{1,n} = \sqrt{k_n^2 - k_{02,n}^2} + O(\delta^2), \quad k_{2,n} = k_{02,n} + \int_{x_0}^{x} \frac{k_n}{\sqrt{k_n^2 - k_{02,n}^2}} \frac{\partial k_n}{\partial y}\,\mathrm{d}\xi + O(\delta^2), \tag{4.18}$$

$$S_n = k_{02,n} y + S_{0,n} + \delta \int_{x_0}^{x} \sqrt{k_n^2 - k_{02,n}^2}\,\mathrm{d}\xi + O(\delta^2), \tag{4.19}$$

and the extension is apparent in (4.18)–(4.19) as a non-constant term in the definition of $k_{2,n}$ and in the dependence of k_n on the y-argument. The definition ($k_{2,n} = k_{02,n} = \text{const.}$) for $O(\delta^0)$, (4.18)–(4.19) for $O(\delta)$ or (4.15)–(4.17) for $O(\delta^2)$ (as well as other solutions of higher accuracy) can be used to provide the definition of $k_{1,n}$, which is needed to complete the linear OPE model (3.15). Hence, the linear OPE is based on the wave ray structure developed in this section. The resulting ray path structure is curved even for the lowest-order solution. This extends the more simplified approach used in various previous works, where a simple rotation of the coordinate system was applied in order to account for the obliqueness of the incident waves while retaining a straight wave ray path approach. This rotation will allow a good representation of the oblique incoming waves in deep water (for a single direction), but as the waves shoal and change their direction, the difference between the straight wave ray assumption and the actual curved wave propagation will produce errors.

The derivation in this section is independent and can be used as the basis for formulating other types of OPEs (such as ones with higher orders of lateral derivatives). Also, it is not limited by the assumption of a mild slope in the x-direction, and yields the same result when setting $\mu = 1$. For an increase in accuracy, (4.8) can be easily extended to higher orders of δ to allow calculation of higher-order κ-terms. Another option for increasing the accuracy of the solution is to use a Padé

https://doi.org/10.1017/jfm.2012.502 Published online by Cambridge University Press

approximation (instead of a Taylor series), which allows us to create a more accurate formulation while using lower-order terms. Note that for the purposes of this work there may be no need for this further increase in accuracy. The reason for this is that bottom slope terms of $O((\partial h/\partial x)^2, (\partial h/\partial y)^2, |(\partial h/\partial x)(\partial h/\partial y)|)$ have already been neglected in the formulation of (3.15), and the wavenumbers change in correspondence to the bottom slope. The relation between the wavenumber derivatives and the bottom slopes, $\nabla k = (\partial k/\partial h)\nabla h$, can be easily calculated through the dispersion relation (2.7) to evaluate whether the higher-order terms are in accordance with the order of the equation. Still, one should take into account that, due to the integration process along the x-axis, small errors may accumulate to produce a lower-order effect of high-order terms. Therefore, for long shoaling scenarios, higher accuracy of wave ray solutions may be required.

5. Derivation of the nonlinear part for forward-propagating waves

Equation (3.15) is a parabolic approximation of the linear part of (2.1) under an assumption of negligible wave reflection $\left(\phi_n^- \backsimeq 0\right)$, which relates to a mild slope approximation. Hence, under the same assumption, a nonlinear parabolic model can be written by substituting the elliptic linear part of (2.1) by its parabolic approximation:

$$2ik_{1,n}\left(CC_g\right)_n \frac{\partial \phi_n}{\partial x} + \left[\left(k_{c,n}^2 + k_{1,n}^2\right)\left(CC_g\right)_n + \mathrm{i}\frac{\partial}{\partial x}\left(k_1 CC_g\right)_n\right]\phi_n + \frac{\partial}{\partial y}\left(\left(CC_g\right)_n \frac{\partial \phi_n}{\partial y}\right) = NL_n. \tag{5.1}$$

As the magnitude of the nonlinear terms is smaller than the linear ones, and the linear wave reflection was assumed to be negligible, it is plausible to deduce that the nonlinear reflection is also negligible. Therefore, the nonlinear part NL_n of (5.1) for the forward-propagating waves does not change from the one used in the elliptic model (equation (2.9)). The same approach is actually applied in any modal forward-propagating model; for hyperbolic, parabolic and Fourier models see Agnon *et al.* (1993), Kaihatu & Kirby (1995) and Janssen *et al.* (2008), respectively.

Let us inspect (5.1). In addition to interactions between waves propagating in different harmonics, one must consider that waves are propagating in different directions. Therefore, each modal potential base function can be written as a sum of directional components:

$$\phi_n(x, y) = \sum_{m=-M}^{M} \phi_{n,m}(x, y), \tag{5.2}$$

where each directional component has a travelling wave structure,

$$\phi_{n,m} \sim B_{n,m} \mathrm{e}^{\mathrm{i}S_{n,m}}. \tag{5.3}$$

Using (5.2)–(5.3) and neglecting terms of $O((ka)^2\,\nabla h)$, the following simplification can be applied to the nonlinear part:

$$\nabla \phi_{l,m_1} \cdot \nabla \phi_{n-l,m_2} \simeq -\left(k_{1,l,m_1} k_{1,n-l,m_2} + k_{2,l,m_1} k_{2,n-l,m_2}\right)\phi_{l,m_1}\phi_{n-l,m_2}, \tag{5.4}$$

$$\nabla \phi^*_{l,m_1} \cdot \nabla \phi_{n+l,m_2} \simeq \left(k_{1,l,m_1} k_{1,n+l,m_2} + k_{2,l,m_1} k_{2,n+l,m_2}\right)\phi^*_{l,m_1}\phi_{n+l,m_2}. \tag{5.5}$$

where $\nabla S_{n,m} \equiv \boldsymbol{k}_{n,m} \equiv (k_{1,n,m}, k_{2,n,m})^{\mathrm{T}}$. Equations (5.4) and (5.5) refer to the nonlinear terms that consist of information on directionality of the interacting waves. In

https://doi.org/10.1017/jfm.2012.502 Published online by Cambridge University Press

previous formulations, where the bottom was also changing in the lateral direction (see e.g. Kaihatu & Kirby 1995; Janssen *et al.* 2008), a small crossing angle was assumed (i.e. $\nabla\phi_l \cdot \nabla\phi_{n-l} = -k_l k_{n-l}\phi_l\phi_{n-l}$ and $\nabla\phi_l^* \cdot \nabla\phi_{n+l} = k_l k_{n-l}\phi_l^*\phi_{n+l}$). Hence, for directional wave spectra, (5.4) and (5.5) present an improvement in the nonlinear representation, which grows as the crossing angle increases. The law of cosines in its vector representation (or simply the definition of the dot product) shows that the ratio between the current approach to the same terms with a small crossing angle assumption is $\boldsymbol{k}_{l,m_1} \cdot \boldsymbol{k}_{n\pm l,m_2}/k_l k_{n\pm l} = \cos(\Delta\theta)$, where $\Delta\theta$ represents the crossing angle between two interacting waves. This shows that for two waves propagating in $\pm 15, \pm 22.5$ and $\pm 30°$, the error of the nonlinear coefficients incorporating the small crossing angle assumption is of ~ 13, ~ 29 and 50 % respectively (see appendix B).

Applying (2.9) and (5.2)–(5.5) to (5.1) yields

$$\begin{aligned}
&\sum_{m_0=-M}^{M} \left\{ 2\mathrm{i}k_{1,n,m_0}\left(CC_g\right)_n \frac{\partial\phi_{n,m_0}}{\partial x} + \frac{\partial}{\partial y}\left(\left(CC_g\right)_n \frac{\partial\phi_{n,m_0}}{\partial y}\right) \right. \\
&\qquad \left. + \left[\left(k_{c,n}^2 + k_{1,n,m_0}^2\right)\left(CC_g\right)_n + \mathrm{i}\frac{\partial}{\partial x}\left(k_{1,n,m_0}\left(CC_g\right)_n\right)\right]\phi_{n,m_0} \right\} \\
&\quad = \frac{\mathrm{i}}{4}\sum_{l=1}^{N-1}\sum_{m_{1,2}=-M}^{M} P^{+}_{(n,l,m_1,m_2)}\phi_{l,m_1}\phi_{n-l,m_2} \\
&\qquad - \frac{\mathrm{i}}{2}\sum_{l=1}^{N-n}\sum_{m_{1,2}=-M}^{M} P^{-}_{(n,l,m_1,m_2)}\phi^*_{l,m_1}\phi_{n+l,m_2}, \qquad (5.6)
\end{aligned}$$

$$\begin{aligned}
P^{\pm}_{(n,l,m_1,m_2)} &= 2\omega_n\left(k_{1,l,m_1}k_{1,n\mp l,m_2} + k_{2,l,m_1}k_{2,n-l,m_2}\right) \\
&\quad + \omega_l k_{n\mp l}^2 \pm \omega_{n-l}k_l^2 - \frac{\omega_l\omega_{n\mp l}\omega_n}{g^2}\left(\omega_l^2 \pm \omega_l\omega_{n\mp l} + \omega_{n\pm l}^2\right). \qquad (5.7)
\end{aligned}$$

Using representations (5.2) and (5.3), the linear equations can be written separately for each wave mode and wave direction together with nonlinear coupling terms, resulting in a quadratic nonlinear OPE model:

$$\begin{aligned}
&2\mathrm{i}k_{1,n,m_0}\left(CC_g\right)_n \frac{\partial\phi_{n,m_0}}{\partial x} + \frac{\partial}{\partial y}\left(\left(CC_g\right)_n \frac{\partial\phi_{n,m_0}}{\partial y}\right) \\
&\qquad + \left[\left(k_{c,n}^2 + k_{1,n,m_0}^2\right)\left(CC_g\right)_n + \mathrm{i}\frac{\partial}{\partial x}\left(k_{1,n,m_0}\left(CC_g\right)_n\right)\right]\phi_{n,m_0} \\
&\quad = \frac{\mathrm{i}}{4}\sum_{l=1}^{N-1}\sum_{m_{1,2}=-M}^{M} P^{+}_{(n,l,m_1,m_2)}\phi_{l,m_1}\phi_{n-l,m_2}\mathscr{D}^{+}_{(n,l,m_0,m_1,m_2)} \\
&\qquad - \frac{\mathrm{i}}{2}\sum_{l=1}^{N-n}\sum_{m_{1,2}=-M}^{M} P^{-}_{(n,l,m_1,m_2)}\phi^*_{l,m_1}\phi_{n+l,m_2}\mathscr{D}^{-}_{(n,l,m_0,m_1,m_2)}. \qquad (5.8)
\end{aligned}$$

Here, $\mathscr{D}^{\pm}$ are decision functions that should require the class III Bragg resonance condition (see Liu & Yue 1998*a*) in the lateral direction to be satisfied. Under the assumption of small lateral changes and small nonlinearity, these functions can be determined in the lowest order simply as

$$\mathscr{D}^{\pm}_{(n,l,m_0,m_1,m_2)} = \delta_{m_2\pm m_1,m_0}, \qquad (5.9)$$

https://doi.org/10.1017/jfm.2012.502 Published online by Cambridge University Press

where $\delta_{i,j}$ is the Kronecker δ (see e.g. Agnon *et al.* 1993; Herbers & Burton 1997). Equation (5.9) expresses the satisfaction of the class III Bragg resonance for the case of no lateral bottom change (see Liu & Yue 1998*b*). Locally, this assumption is consistent with the order of the nonlinear part, as terms of $O((ka)^2\,|\partial h/\partial y|)$ have already been neglected. From an integral point of view, the underlying assumption is that the energy of the wave components does not alter much near the ray solution. This assumption actually exists in any quadratic nonlinear parabolic model, while using only one wave direction component along the x-axis ($M = 0$) and assuming a straight wave ray solution for each wave mode.

Equation (5.8) is a quadratic nonlinear oblique parabolic equation for each wave direction (m_0) and wave harmonic (n). The complete set of equations forms the nonlinear oblique parabolic equation model. In the case of taking only the normal incident wave assumption (i.e. $k_2 = 0$ and $M = 0$), (5.8) represents an N-equation parabolic model such as that derived by Kaihatu & Kirby (1995). It differs in the use of local wavenumber quantities with the perturbation solution to a chosen order, rather than using laterally averaged quantities while neglecting lateral derivatives of the wavenumbers.

For the case of one-dimensional wave shoaling, (5.8) reduces to

$$2\mathrm{i}\left(kCC_g\right)_n\frac{\partial\phi_n}{\partial x}+\left[2k_n^2\left(CC_g\right)_n+\mathrm{i}\frac{\partial}{\partial x}\left(\left(kCC_g\right)_n\right)+\bar{r}_n\nabla^2 h\right]\phi_n$$
$$=\frac{\mathrm{i}}{4}\sum_{l=1}^{N-1}P^{+}_{(n,l)}\phi_l\phi_{n-l}-\frac{\mathrm{i}}{2}\sum_{l=1}^{N-n}P^{-}_{(n,l)}\phi_l^{*}\phi_{n+l}, \tag{5.10}$$

$$P^{\pm}_{(n,l)}=2\omega_n k_l k_{n\mp l}+\omega_l k_{n\mp l}^2\pm\omega_{n-l}k_l^2-\frac{\omega_l\omega_{n\mp l}\omega_n}{g^2}(\omega_l^2\pm\omega_l\omega_{n\mp l}+\omega_{n\pm l}^2). \tag{5.11}$$

Equation (5.10) coincides with the models of Agnon *et al.* (1993) and Kaihatu & Kirby (1995) in their one-dimensional formulations by neglecting the bottom curvature term and substituting the wave structure

$$\phi_n=\frac{-\mathrm{i}g}{\omega_n}a_n\mathrm{e}^{\mathrm{i}\int k_n\mathrm{d}x}. \tag{5.12}$$

6. The second-order relation between the velocity potential and the surface elevation

6.1. *Defining the surface elevation base functions in terms of the velocity potential ones*

In (5.12), a_n represents the amplitude of the surface elevation where linear relations between the velocity potential and the surface elevation amplitudes were used. Eldeberky & Madsen (1999) showed that for consistency, second-order relations between the amplitudes should be taken (see also Kaihatu 2001; Bredmose *et al.* 2005). In order to do so, the derivation will follow that of Eldeberky & Madsen (1999), but with the notation used in this paper with an extension to the two-dimensional nature of the problem.

The full free-surface dynamic boundary condition for free-surface gravity waves is given by

$$\frac{\partial\Phi}{\partial t}+g\eta+\frac{1}{2}\left|\nabla\Phi\right|^2+\frac{1}{2}\left(\frac{\partial\Phi}{\partial z}\right)^2=0,\quad z=\eta. \tag{6.1}$$

https://doi.org/10.1017/jfm.2012.502 Published online by Cambridge University Press

Since only second-order relations are required, (6.1) can be written for the undisturbed surface using Taylor expansion in the form

$$\frac{\partial \Phi}{\partial t} + g\eta + \frac{1}{2}|\nabla \Phi|^2 + \frac{1}{2}\left(\frac{\partial \Phi}{\partial z}\right)^2 + \eta \frac{\partial^2 \Phi}{\partial z \partial t} = O((ka)^3), \quad z = 0. \tag{6.2}$$

From (6.2) the following expression for η can be found:

$$\eta = -\frac{1}{g}\frac{\partial \Phi}{\partial t} - \frac{1}{2g}|\nabla \Phi|^2 - \frac{1}{2g}\left(\frac{\partial \Phi}{\partial z}\right)^2 + \frac{1}{g^2}\frac{\partial \Phi}{\partial t}\frac{\partial^2 \Phi}{\partial z \partial t} + O((ka)^3), \quad z = 0, \tag{6.3}$$

where the wave elevation in the nonlinear part was written in terms of the velocity potential using the linear relation from the same equation.

Let us describe the surface elevation using a superposition of solutions as follows:

$$\eta = \frac{1}{2}\sum_{n=1}^{N}\sum_{m=-M}^{M}\left[\eta_{n,m}(x,y)\mathrm{e}^{-\mathrm{i}\omega_n t} + \eta^*_{n,m}(x,y)\mathrm{e}^{\mathrm{i}\omega_n t}\right]. \tag{6.4}$$

Applying (2.5), (2.6), (5.2) and (6.4) to (6.3) yields after some manipulation

$$\begin{aligned}\eta_{n,m_0} = {} & \frac{\mathrm{i}\omega_n}{g}\phi_{n,m_0} + \frac{1}{4g^3}\sum_{l=1}^{n-1}\sum_{m_{1,2}=-M}^{M} T^{+}_{(n,l,m_1,m_2)}\phi_{l,m_1}\phi_{n-l,m_2}\mathscr{D}^{+}_{(n,l,m_0,m_1,m_2)} \\ & - \frac{1}{2g^3}\sum_{l=1}^{N-n}\sum_{m_{1,2}=-M}^{M} T^{-}_{(n,l,m_1,m_2)}\phi^*_{l,m_1}\phi_{n+l,m_2}\mathscr{D}^{-}_{(n,l,m_0,m_1,m_2)},\end{aligned} \tag{6.5}$$

$$T^{+}_{(n,l,m_1,m_2)} = g^2\left(k_{1,l,m_1}k_{1,n-l,m_2} + k_{2,l,m_1}k_{2,n-l,m_2}\right) - \omega_l^2\omega_{n-l}^2 - 2\omega_l\omega_{n-l}^3, \tag{6.6}$$

$$T^{-}_{(n,l,m_1,m_2)} = g^2\left(k_{1,l,m_1}k_{1,n+l,m_2} + k_{2,l,m_1}k_{2,n+l,m_2}\right) + \omega_l^2\omega_{n+l}^2 - \omega_l\omega_{n+l}\left(\omega_l^2 + \omega_{n+l}^2\right). \tag{6.7}$$

Equations (6.5)–(6.7) present the relation between the modal and directional surface elevation to the velocity potential ones. A detailed derivation of this equation is given in appendix A.

In the case of one-dimensional propagation, equations (6.5)–(6.7) reduce to

$$\begin{aligned}\eta_n = {} & \frac{\mathrm{i}\omega_n}{g}\phi_n - \frac{1}{2g^3}\sum_{l=1}^{N-n}\left(g^2k_lk_{n+l} + \omega_l^2\omega_{n+l}^2 - \omega_l\omega_{n+l}\left(\omega_l^2 + \omega_{n+l}^2\right)\right)\phi_l^*\phi_{n+l} \\ & + \frac{1}{4g^3}\sum_{l=1}^{n-1}\left(g^2k_lk_{n-l} - \omega_l^2\omega_{n-l}^2 - 2\omega_l\omega_{n-l}^3\right)\phi_l\phi_{n-l}.\end{aligned} \tag{6.8}$$

6.2. *The nonlinear oblique parabolic model in terms of the surface elevation*

In order to construct evolution equations in terms of the surface-elevation amplitude, it is first necessary to write the definition of the velocity potential in term of the surface elevation. This can be done by substituting the linear relation for the nonlinear part

https://doi.org/10.1017/jfm.2012.502 Published online by Cambridge University Press

of (6.5), which results in

$$\frac{\mathrm{i}\omega_n}{g}\phi_{n,m_0} = \eta_{n,m_0} + \frac{1}{4g}\sum_{l=1}^{n-1}\sum_{m_{1,2}=-M}^{M}\frac{1}{\omega_l\omega_{n-l}}T^{+}_{(n,l,m_1,m_2)}\eta_{l,m_1}\eta_{n-l,m_2}\mathscr{D}^{+}_{(n,l,m_0,m_1,m_2)} + \frac{1}{2g}\sum_{l=1}^{N-n}\sum_{m_{1,2}=-M}^{M}\frac{1}{\omega_l\omega_{n+l}}T^{-}_{(n,l,m_1,m_2)}\eta^{*}_{l,m_1}\eta_{n+l,m_2}\mathscr{D}^{-}_{(n,l,m_0,m_1,m_2)}. \tag{6.9}$$

Equation (6.9) can then be substituted for (5.8), where in its nonlinear part the linear relations are sufficient. This yields the nonlinear OPE model in terms of the surface elevation:

$$\begin{aligned}&2\mathrm{i}k_{1,n,m_0}\left(CC_g\right)_n\frac{\partial\eta_{n,m_0}}{\partial x} + \frac{\partial}{\partial y}\left(\left(CC_g\right)_n\frac{\partial\eta_{n,m_0}}{\partial y}\right)\\ &\quad + \left[\left(k^2_{c,n}+k^2_{1,n,m_0}\right)\left(CC_g\right)_n + \mathrm{i}\frac{\partial}{\partial x}\left(k_{1,n,m_0}\left(CC_g\right)_n\right)\right]\eta_{n,m_0}\\ &= \frac{1}{4g}\sum_{l=1}^{N-1}\sum_{m_{1,2}=-M}^{M}Q^{+}_{(n,l,m_0,m_1,m_2)}\eta_{l,m_1}\eta_{n-l,m_2}\mathscr{D}^{+}_{(n,l,m_0,m_1,m_2)}\\ &\quad + \frac{1}{2g}\sum_{l=1}^{N-n}\sum_{m_{1,2}=-M}^{M}Q^{-}_{(n,l,m_0,m_1,m_2)}\eta^{*}_{l,m_1}\eta_{n+l,m_2}\mathscr{D}^{-}_{(n,l,m_0,m_1,m_2)},\end{aligned} \tag{6.10}$$

$$\begin{aligned}Q^{\pm}_{(n,l,m_0,m_1,m_2)} &= \Big[2k_{1,n,m_0}\left(k_{1,n\mp l,m_2}\pm k_{1,l,m_1}\right) - \left(k_n^2+k^2_{1,n,m_0}\right)\\ &\quad + \left(k_{2,n\mp l,m_2}\pm k_{2,l,m_1}\right)^2\Big]\frac{\left(CC_g\right)_n}{\omega_l\omega_{n\mp l}}T^{\pm}_{(n,l,m_1,m_2)} + \frac{\omega_n g^2}{\omega_l\omega_{n\mp l}}P^{\pm}_{(n,l,m_1,m_2)}.\end{aligned} \tag{6.11}$$

The nonlinear coefficients given in (6.11) can be further simplified by taking into account the small lateral changes and (5.9), to yield

$$\begin{aligned}Q^{\pm}_{(n,l,m_0,m_1,m_2)} &= \frac{\omega_n g^2}{\omega_l\omega_{n\mp l}}P^{\pm}_{(n,l,m_1,m_2)}\\ &\quad + 2k_{1,n,m_0}\left(k_{1,n\mp l,m_2}\pm k_{1,l,m_1}-k_{1,n,m_0}\right)\frac{\left(CC_g\right)_n}{\omega_l\omega_{n\mp l}}T^{\pm}_{(n,l,m_1,m_2)}.\end{aligned} \tag{6.12}$$

The one-dimensional model in terms of the surface elevation is hence given by

$$\begin{aligned}&2\mathrm{i}\left(kCC_g\right)_n\frac{\partial\eta_n}{\partial x} + \left[2k_n^2\left(CC_g\right)_n + \mathrm{i}\frac{\partial}{\partial x}\left(\left(kCC_g\right)_n\right) + \bar{r}_n\nabla^2 h\right]\eta_n\\ &\quad = \frac{1}{4g}\sum_{l=1}^{N-1}Q^{+}_{(n,l)}\eta_l\eta_{n-l} + \frac{1}{2g}\sum_{l=1}^{N-n}Q^{-}_{(n,l)}\eta^{*}_l\eta_{n+l},\end{aligned} \tag{6.13}$$

$$Q^{\pm}_{(n,l)} = 2k_n\left(k_{n\mp l}\pm k_l-k_n\right)\frac{\left(CC_g\right)_n}{\omega_l\omega_{n\mp l}}T^{\pm}_{(n,l)} + \frac{\omega_n g^2}{\omega_l\omega_{n\mp l}}P^{\pm}_{(n,l)}. \tag{6.14}$$

The difference between the one-dimensional nonlinear coefficients, with and without taking into account the nonlinear amplitude relations, is presented in figure 1.

https://doi.org/10.1017/jfm.2012.502 Published online by Cambridge University Press

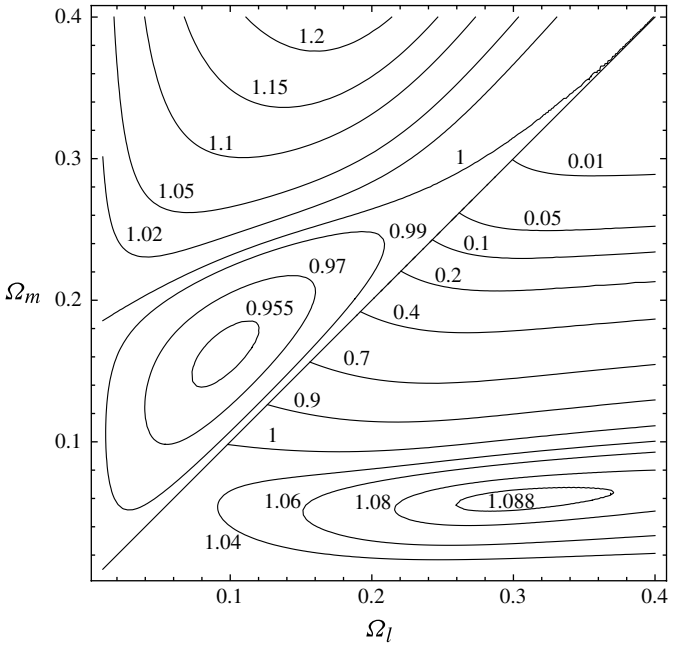


FIGURE 1. The influence of the second-order corrections on the nonlinear interaction coefficients. Contour plot of the ratio $Q^{\pm}|_{T^{\pm}=0}/Q^{\pm}$ as given in (6.14) for one-dimensional interactions. The ratios for Q^{+} and Q^{-} are given below and above the diagonal respectively. The arguments are $\Omega_l = (\omega_l/2\pi)\sqrt{h/g}$ and $\Omega_m = (\omega_{n\mp l}/2\pi)\sqrt{h/g}$, in which the $\mp$ sign relates to $Q^{\pm}$.

7. Numerical calculations

Numerical calculations are presented in this section for both linear and nonlinear wave shoaling. The nonlinear mild-slope equation was calculated using (2.1) and (2.9), together with the following definition:

$$\phi_n(x, y) = \sum_{m=-M}^{M} \varphi_n(x) \mathrm{e}^{\mathrm{i}k_{02,m}y}. \tag{7.1}$$

This definition suits the quasi-two-dimensional nature of the problems considered, which reduces the equation to one dimension. The linear numerical integrations as well as the nonlinear ones were computed using the NDSolve function of the Mathematica 8 software. The mild-slope equation was solved using two boundary conditions of a propagating wave at $x = 0$.

The higher-order term R_n is not taken into account in the numerical calculations. Its high-order gradient components ($|\nabla h|^2$) have already been shown to be insignificant for the relevant shoaling problems due to the assumption of negligible reflection (actually the reduction of the elliptic mild-slope equation to a single parabolic equation demands that this term is negligible: see § 3). The bottom curvature ($\nabla^2 h$) was shown to have a significant effect on shoaling problems for problems with wave reflection (see Chamberlain & Porter 1995). Note that for a reflection coefficient of value lower than 10^{-1}, the effect of these terms on the reflection was insignificant for the Booij ramp test case (unfortunately, the effect on the transmitted wave, if any, is

https://doi.org/10.1017/jfm.2012.502 Published online by Cambridge University Press

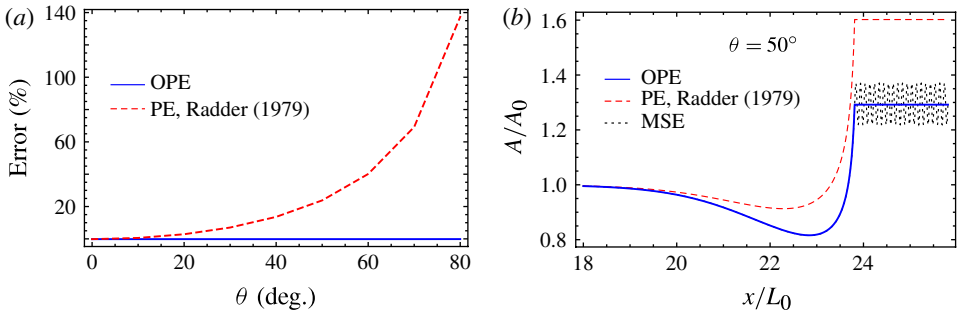


FIGURE 2. (Colour online) *(a)* The shoaling error of an oblique incident monochromatic wave with respect to its attack angle. The incident wave is of period $T = 2$ s propagating over a $1/10$ bottom slope without lateral changes, ending with a plateau at depth $kh = 0.2$. Dashed red line, the parabolic equation (PE) of Radder (1979); solid blue line, the oblique parabolic model (equation (3.15)). *(b)* The normalized wave amplitude for a $\theta = 50^\circ$ oblique incident wave. L_0 represents the deep-water wavelength. Dashed and solid lines as in (*a*); dotted black line, a solution using the mild-slope equation (MSE) of Berkhoff (1972).

not described). Some experimental tests made on the linear shoaling over a parabolic mount (not shown here), presented negligible contribution of the higher-order term R_n to the oblique parabolic equation ($\sim 10^{-6} - 10^{-7}$ effect on the normalized wave height). In order to keep the numerical problems simple, the bottom profiles used in this section will comprise a linearly sloping bottom ending with a plateau. Including the curvature terms will require an additional analytical derivation to construct the appropriate jump conditions. This derivation will remain beyond the scope of this paper. Hence, the contribution of the bottom curvature has been neglected both in the OPE models and, for consistency, also in the linear and nonlinear mild-slope equation models, which were used as the target benchmarks.

7.1. *Linear shoaling of oblique incident waves*

Numerical calculations are presented in this subsection in order to confirm the quantitative benefits of using the linear OPE (3.15) in the case of linear oblique incident waves. The bottom profiles of the numerical experiments are taken as linear $1/10$ and $1/5$ bottom slopes without lateral changes, starting in deep water ending with a plateau at depth $kh = 0.2$. The incident wave is of period $T = 2$ s with a changing attack angle.

In order to identify the advantage of the oblique parabolic equation with respect to the attack angle of the oblique incident waves, it is compared to the parabolic equation of Radder (1979) and the mild-slope equation (the linear part of (2.1) with $R_n = 0$). Numerical results of the shoaling problem with waves approaching from different incident angles are given in figure 2. The errors of the two parabolic equations compared to the average wave height of the mild-slope equation on the plateau for the milder $1/10$ slope are presented in figure 2(*a*). The normalized wave amplitude solution of each of the models for $\theta_i = 50^\circ$ initial oblique incidence waves are presented in figure 2(*b*). Figure 3 presents the same comparison but for the steeper $1/5$ slope. It can be seen that as the attack angle increases the improvement becomes more significant. It should be noted that, in this case, the models of Liu & Tsay (1985) are expected to produce the same successful solution as the linear OPE. This should be the case because the averaged bottom in the case of no lateral bottom changes

https://doi.org/10.1017/jfm.2012.502 Published online by Cambridge University Press

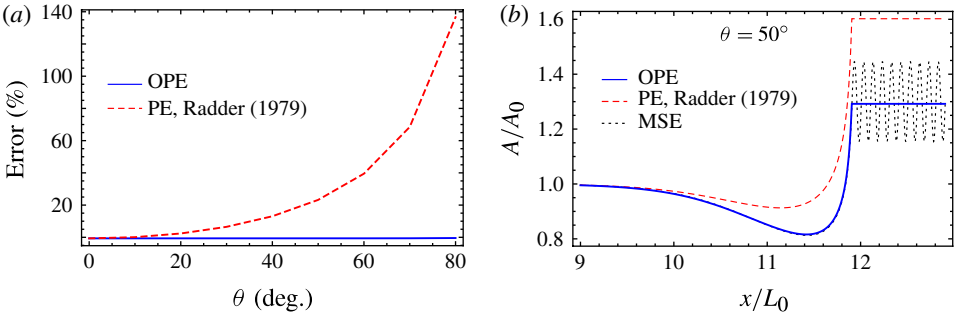


FIGURE 3. (Colour online) The same as figure 2 but for a 1/5 bottom slope.

coincides with the local depth used in the lowest-order perturbation solution. Moreover, the higher-order perturbation corrections are not required in this case, as the lateral derivative of the wavenumber is zero. This is also true for the model of Dalrymple & Kirby (1988), as the averaged depth relates to the constant term in the Fourier transform.

7.2. *Nonlinear shoaling of oblique incident waves: single wave*

Numerical calculations are presented in this subsection in order to confirm the accuracy of the nonlinear OPE (5.8) in the case of oblique incident waves and give physical insight into the nonlinear shoaling of a single wave harmonic. The bottom profile of the numerical experiment is taken as a linear 1/5 bottom slope without lateral changes, starting in deep water and ending with a plateau at depth $h = 0.4$ m ($kh \simeq 0.68$). The incident wave is of period $T = 2$ s with an attack angle of $\theta_i = 25°$ and a starting nonlinearity of $k_0 A_0 = 0.03$. The equation set was truncated at $M = N = 4$.

Figures 4(*a*)–4(*c*) present the normalized amplitude of $\phi_{1,1}$, $\phi_{2,2}$ and $\phi_{3,3}$ respectively. As expected, the super-harmonic interactions transfer energy to the second and third harmonics (and so on) of double and triple (and so on) values in the lateral wavenumber respectively. Figure 4(*d*) shows the change in direction of the participating wave components (the same for each model). These angles were simply calculated using the formula $\arcsin\left(k_{02,m}/k_n\right)$ Here, the first and second harmonics refract, and the third harmonic does not change its direction, since compared to its wavelength, the bottom is too deep for such an effect. The results of the super-harmonic wave interactions are in excellent agreement with those of the nonlinear mild-slope equation (calculated using (2.1), (2.9) and (7.1) for each wave direction and mode).

7.3. *Nonlinear shoaling of oblique incident waves: two waves*

Numerical calculations are presented in this subsection in order to confirm the accuracy of the nonlinear oblique parabolic (5.8) in the case of directional wave interactions and give physical insight into the nonlinear shoaling of two monochromatic waves initiating from different angles. The bottom profile of the numerical experiments is taken as the one used in § 7.2. Two oblique incident waves of period $T = 2$ s and starting nonlinearity $k_0 A_0 = 0.03$ are approaching at attack angles of $\theta_i = \pm 15°$. The equation set calculating this interaction was also truncated

https://doi.org/10.1017/jfm.2012.502 Published online by Cambridge University Press

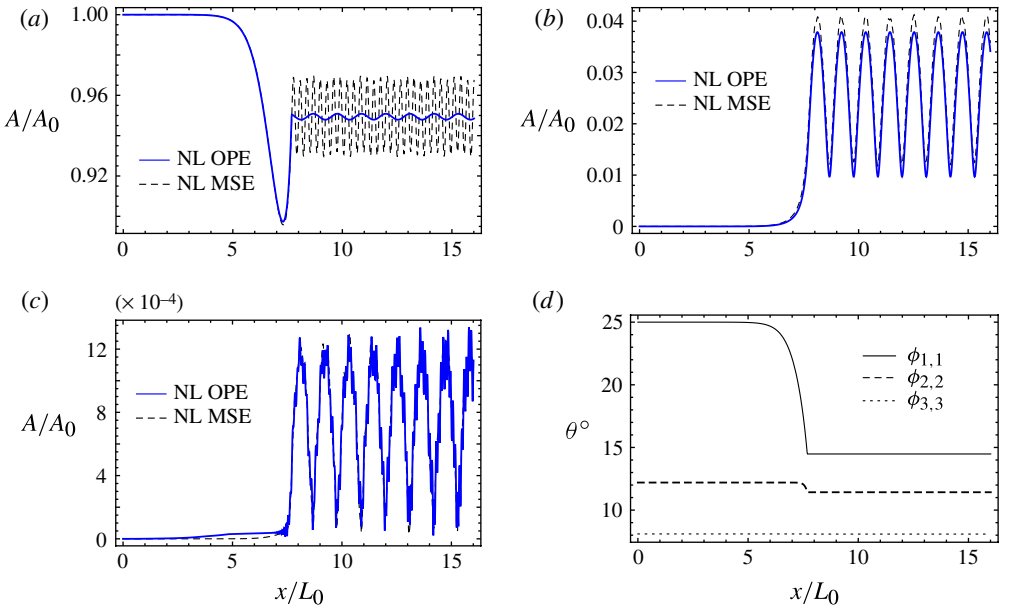


FIGURE 4. (Colour online) The nonlinear shoaling of an oblique incident wave approaching at an attack angle of $\theta = 25°$. The incident wave, which is of period $T = 2$ s and nonlinearity $kA = 0.03$, propagate over a 1/5 bottom slope without lateral changes, ending with a plateau in $kh \simeq 0.68$. The velocity potential amplitudes are normalized using the deep-water incident amplitude. L_0 represents the first-harmonic deep-water wavelength. Dashed black line, the nonlinear mild-slope equations (2.1) and (2.9) of Kaihatu & Kirby (1995); solid blue line, the nonlinear oblique parabolic model (equation (5.8)). The directions of the wave components $\phi_{1,1}$, $\phi_{2,2}$ and $\phi_{3,3}$ (the same for each model) are presented using solid, dashed and dotted black lines respectively: (*a*) $\phi_{1,1}$; (*b*) $\phi_{2,2}$; (*c*) $\phi_{3,3}$; (*d*) wave direction.

at $M = N = 4$. Due to the symmetry of the problem with respect to the x-axis, the results have the property $\phi_{n,m} = \phi_{n,-m}$.

Figure 7 presents the normalized amplitudes of $\phi_{1,\pm1}$, $\phi_{1,\pm3}$, $\phi_{2,0}$, $\phi_{2,\pm2}$, $\phi_{3,\pm1}$ and $\phi_{3,\pm3}$. Figures 8 and 9 present the results for the same problem but with period $T = 3$ s (attack angles $\theta = \pm 10°$). As expected, the super-harmonic self-interactions of the two incident waves ($\phi_{1,\pm1}$) transfer energy to the second and third harmonics of double and triple values in the lateral wavenumber respectively ($\phi_{2,\pm2}$, $\phi_{3,\pm3}$). The sub-harmonic interaction between $\phi_{2,\pm2}$ and $\phi_{1,\mp1}$ results in energy transfer to the $\phi_{1,\pm3}$ component. The super-harmonic interaction between the two incident waves transfer energy to the second harmonic in the normal direction. This wave in turn interacts with the two first-harmonic incident waves to create third-harmonic waves propagating $\phi_{3,\pm1}$. Again, the nonlinear interactions are in very good agreement with those of the nonlinear mild-slope equation. It is also apparent that the previously used assumption of small crossing angles significantly reduces the accuracy of the nonlinear interactions. As described in § 5, this assumption depends on the cosine of the crossing angle ($\cos(\Delta\theta)$). In the present calculation the starting crossing angle for $\phi_{1,\pm1}$ is $\Delta\theta_i = 30°$, and for the main waves it reduces during the shoaling process to $\Delta\theta \simeq 17.6°$. It can be seen that in this case, the results can suffer up to ∼40 % error

https://doi.org/10.1017/jfm.2012.502 Published online by Cambridge University Press

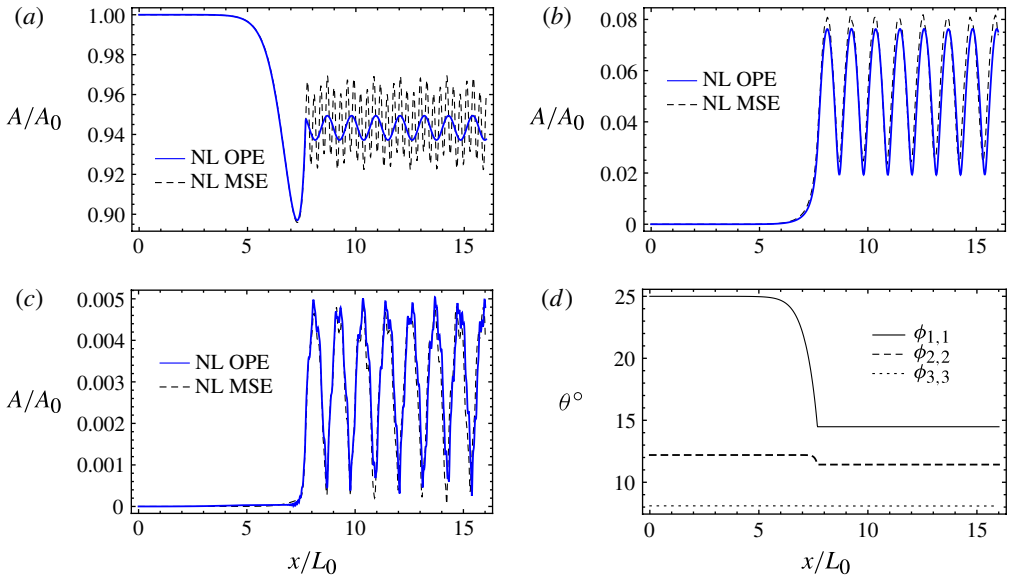


FIGURE 5. (Colour online) The same as figure 4 but for nonlinearity $kA = 0.06$: (*a*) $\phi_{1,1}$; (*b*) $\phi_{2,2}$; (*c*) $\phi_{3,3}$; (*d*) wave direction.

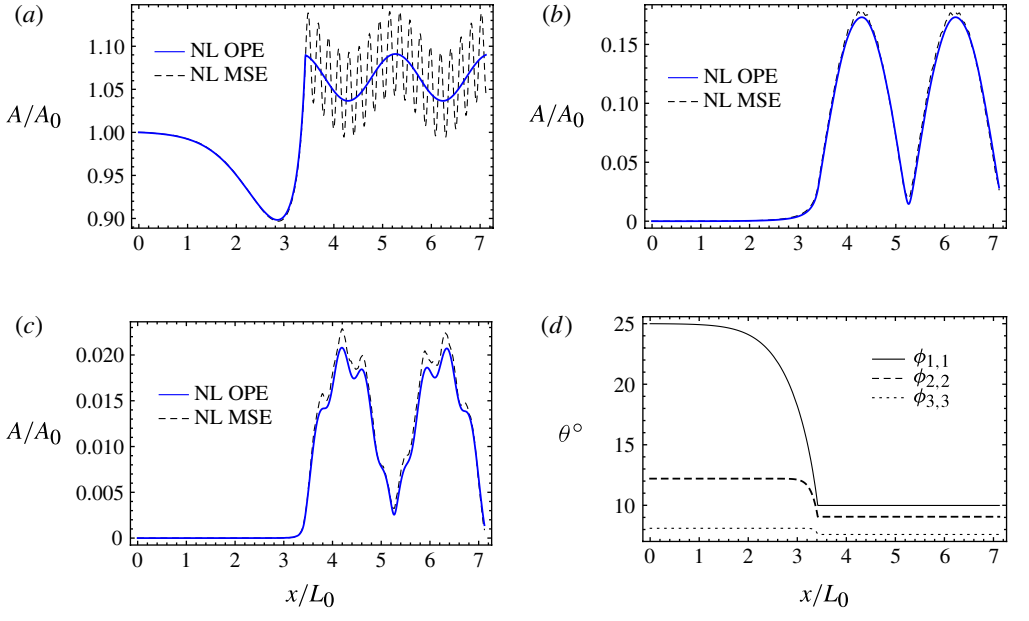


FIGURE 6. (Colour online) The same as figure 4 but for period $T = 3$ s with a plateau in $kh \simeq 0.44$: (*a*) $\phi_{1,1}$; (*b*) $\phi_{2,2}$; (*c*) $\phi_{3,3}$; (*d*) wave direction.

in the accuracy of the higher-order components due to this simplification. As expected, this error reduces (see figure 9) when the starting crossing angle for $\phi_{1,\pm1}$ is smaller (in this case $\Delta\theta_i = 20^\circ$).

https://doi.org/10.1017/jfm.2012.502 Published online by Cambridge University Press

Figure 10 presents the attack angles of the wave components $\phi_{1,1}$, $\phi_{1,3}$, $\phi_{2,2}$ and $\phi_{3,3}$ along the shoaling process (the same for each model). These angles were simply calculated using the formula $\arcsin\left(k_{02,m}/k_n\right)$. Due to the symmetric nature of the problem, the attack angles of the wave components $\phi_{1,-1}$, $\phi_{1,-3}$, $\phi_{2,-2}$ and $\phi_{3,-3}$ are simply the negative angles of their corresponding positive index components. An interesting phenomenon can be seen by observing the $\phi_{1,\pm3}$ wave components of these simple nonlinear wave shoaling problems. It actually propagates in larger attack angles than the original two first-harmonic incident waves. This is counter-intuitive. In linear wave shoaling problems, the waves reduce their attack angle in the refraction process. In the nonlinear shoaling process, however, it is clearly seen that the attack angle of some of the wave energy can actually increase.

8. Summary and discussion

The current work produces a parabolic equation for surface gravity waves based on a forward-propagating wave assumption with a curved ray structure rather than on one with a straight ray in the direction of the main propagation axis. The oblique incident forward-propagating wave ray structures were defined using a perturbation solution of the wavenumber field while assuming small lateral bottom changes. The equation was extended to account for quadratic nonlinear wave interactions that can more accurately deal with large crossing angles.

In the lowest perturbation order, the linear model relates to the solution of oblique incident waves on a bottom with no lateral changes. In fact, in this simple case, when neglecting higher-order bottom terms, the OPE coincides with the geometric optic equation. This can be easily shown by substituting (7.1) for (3.15). Then, the equation can be multiplied by φ^*/ω and added to its complex conjugate to yield

$$\frac{\partial}{\partial x}\left(\frac{k_1}{k}C_g\mathcal{N}\right)=0, \quad \mathcal{N}=|\varphi|^2/\omega, \tag{8.1}$$

for each wave mode and direction.

Equation (8.1) is the corresponding wave action equation for this problem with $\mathcal{N}$ defined as the wave action. Various other linear parabolic formulations fail in retaining the results of (8.1) and produce very large errors (see Johnson & Poulin 2000). And indeed, numerical results of the OPE for oblique incident waves show significant improvements, which increase considerably with respect to the increase in the attack angle. The accuracy of the OPE for the case of general bottom profiles that change in the lateral direction can be extended by using higher orders of the perturbation solution. Still, even using the lowest-order perturbation approach results in a much better wave ray structure assumption than the normally incident one, as the deviation from it can be significantly smaller than the deviation from the positive x-axis.

The present approach is not limited to the derived parabolic model. It can be adapted to other types of parabolic approximations in order to create other oblique parabolic equations, such as those with higher-order lateral and mixed derivatives and those using the minimax approach to augment the linear part of the OPE.

The OPE model was also extended to quadratic nonlinearity. Splitting each harmonic to a sum of various propagation directions enabled extension of the model to account for nonlinear wave shoaling without the limiting assumption of small crossing angles between the interacting waves. The error induced by the small crossing angle assumption used in previous works was evaluated. This assumption was avoided in the present derivation, resulting in significant improvement in the results of the

https://doi.org/10.1017/jfm.2012.502 Published online by Cambridge University Press

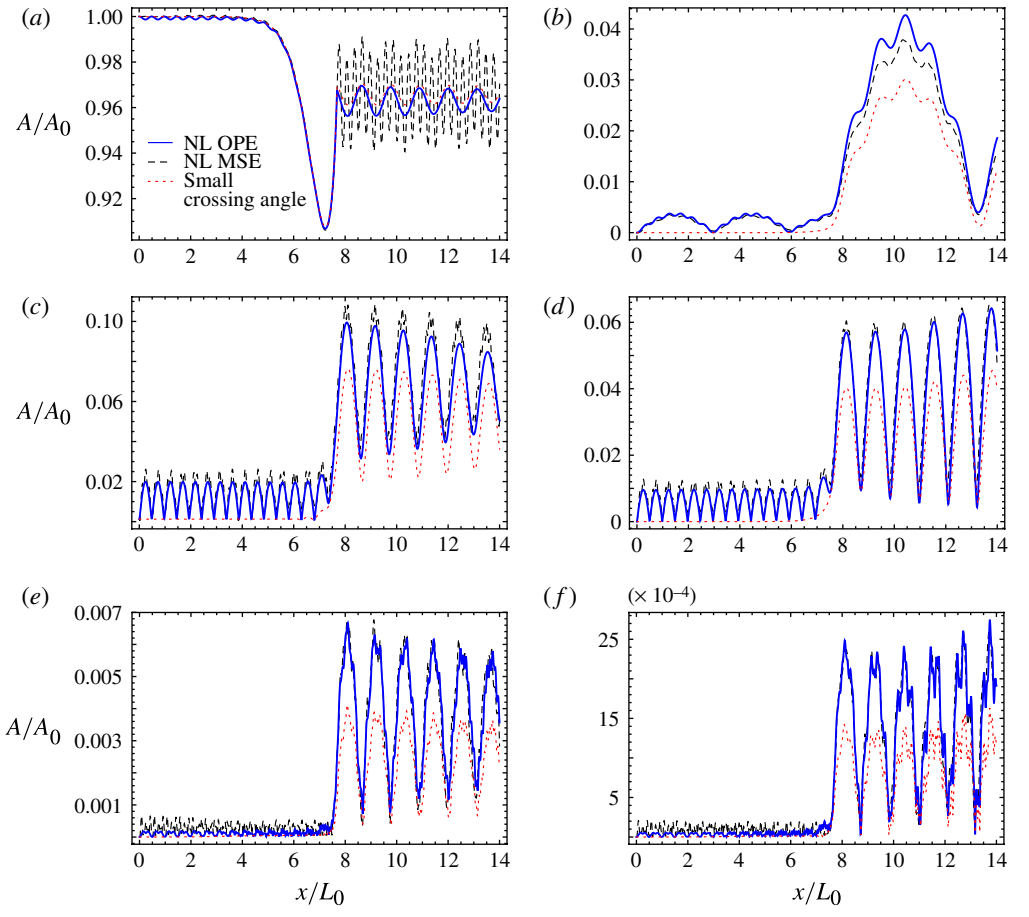


FIGURE 7. (Colour online) The nonlinear shoaling of two oblique incident waves approaching from deep water at attack angles of $\theta = \pm 15°$. The incident waves, which are of period $T = 2$ s and nonlinearity $kA = 0.03$, propagate over a 1/5 bottom slope without lateral changes, ending with a plateau of $kh \simeq 0.68$. The velocity potential amplitudes are normalized using the deep-water incident amplitude. L_0 represents the first-harmonic deep-water wavelength. Dashed black line, the nonlinear mild-slope equations (2.1) and (2.9) of Kaihatu & Kirby (1995); solid blue line, the nonlinear oblique parabolic model (equation (5.8)); dotted red line, the nonlinear oblique parabolic model with a commonly used assumption of small crossing angles (i.e. $\nabla\phi_l \cdot \nabla\phi_{n-l} = -k_l k_{n-l}\phi_l\phi_{n-l}$ and $\nabla\phi_l^* \cdot \nabla\phi_{n+l} = k_l k_{n+l}\phi_l^*\phi_{n+l}$ instead of $\nabla\phi_l \cdot \nabla\phi_{n-l} = -\boldsymbol{k}_l \cdot \boldsymbol{k}_{n-l}\phi_l\phi_{n-l}$ and $\nabla\phi_l^* \cdot \nabla\phi_{n+l} = \boldsymbol{k}_l \cdot \boldsymbol{k}_{n+l}\phi_l^*\phi_{n+l}$ respectively): (*a*) $\phi_{1,1} = \phi_{1,-1}$; (*b*) $\phi_{1,3} = \phi_{1,-3}$; (*c*) $\phi_{2,0}$; (*d*) $\phi_{2,2} = \phi_{2,-2}$; (*e*) $\phi_{3,1} = \phi_{3,-1}$; (*f*) $\phi_{3,3} = \phi_{3,-3}$.

nonlinear model. The nonlinear OPE model showed itself to be sufficiently accurate at reproducing the results of the nonlinear mild-slope equation for wave shoaling in the case of negligible wave reflection, and can be used as a simple alternative method for solving such problems. Basic nonlinear shoaling problems of directional monochromatic waves were investigated using this model. This investigation showed that nonlinear wave shoaling may divert energy to larger attack angles, whereas in the linear framework the waves reduce their attack angle in the shoaling process.

It is worthwhile explaining this phenomenon as it is contrary to linear wave shoaling intuition. For this purpose let us first investigate this process theoretically via the

https://doi.org/10.1017/jfm.2012.502 Published online by Cambridge University Press

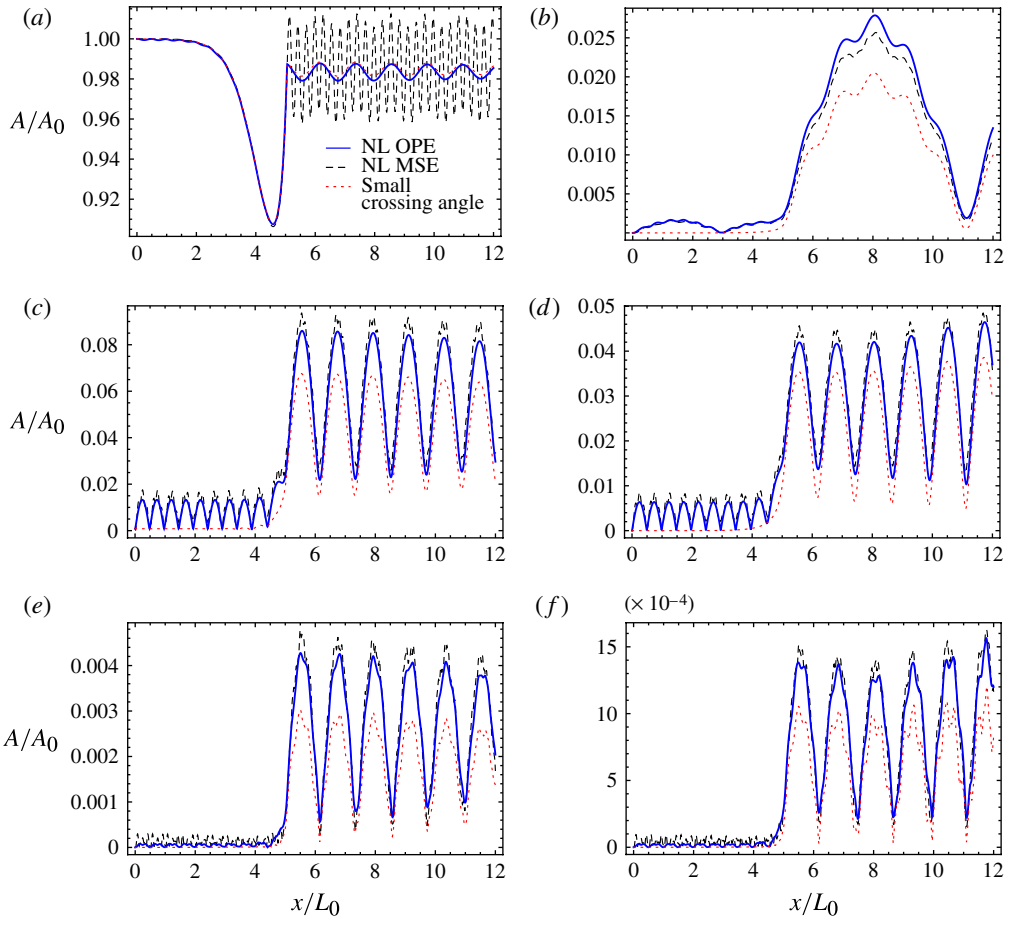


FIGURE 8. (Colour online) The same as figure 7 but for period $T = 3$ s with a plateau in $kh \simeq 0.64$: (*a*) $\phi_{1,1} = \phi_{1,-1}$; (*b*) $\phi_{1,3} = \phi_{1,-3}$; (*c*) $\phi_{2,0}$; (*d*) $\phi_{2,2} = \phi_{2,-2}$; (*e*) $\phi_{3,1} = \phi_{3,-1}$; (*f*) $\phi_{3,3} = \phi_{3,-3}$.

numerical example given in figure 7. Two incident waves ($\phi_{1,\pm1}$) are approaching from deep water at attack angles of $\theta_i = \pm 15°$. The shoaling process of $\phi_{1,1}$ transfers energy via a nonlinear super-harmonic self-interaction to its double-harmonic component $\phi_{2,2}(=\phi_{1+1,1+1})$ propagating at an angle of $\sim 7.5°$. This shorter wave does not feel the bottom for most of the shoaling region (it changes its direction through linear shoaling by $\sim 0.5°$). Nevertheless, via a nonlinear sub-harmonic interaction with the negative angled incident wave $\phi_{1,-1}$, it creates a first-harmonic wave $\phi_{1,3}(=\phi_{2-1,2-(-1)})$. As can be seen in figure 10, this resulting wave propagates at an angle that spans between ~ 27 and $51°$. At the end of the shoaling process the main positive incident wave $\phi_{1,1}$ is propagating at an angle of $\sim 8.8°$. The other positive first-harmonic wave $\phi_{1,3}$ propagates at an angle of $\sim 27°$, which is larger than the initial incident wave angle of $15°$. Due to the symmetry of the problem, the same process happens in the negative angle. The wave energy, which in deep water has been distributed in a directional range of $30°(\pm 15°)$, broadens its directional range to $54°(\pm 27°)$ via the nonlinear shoaling process.

https://doi.org/10.1017/jfm.2012.502 Published online by Cambridge University Press

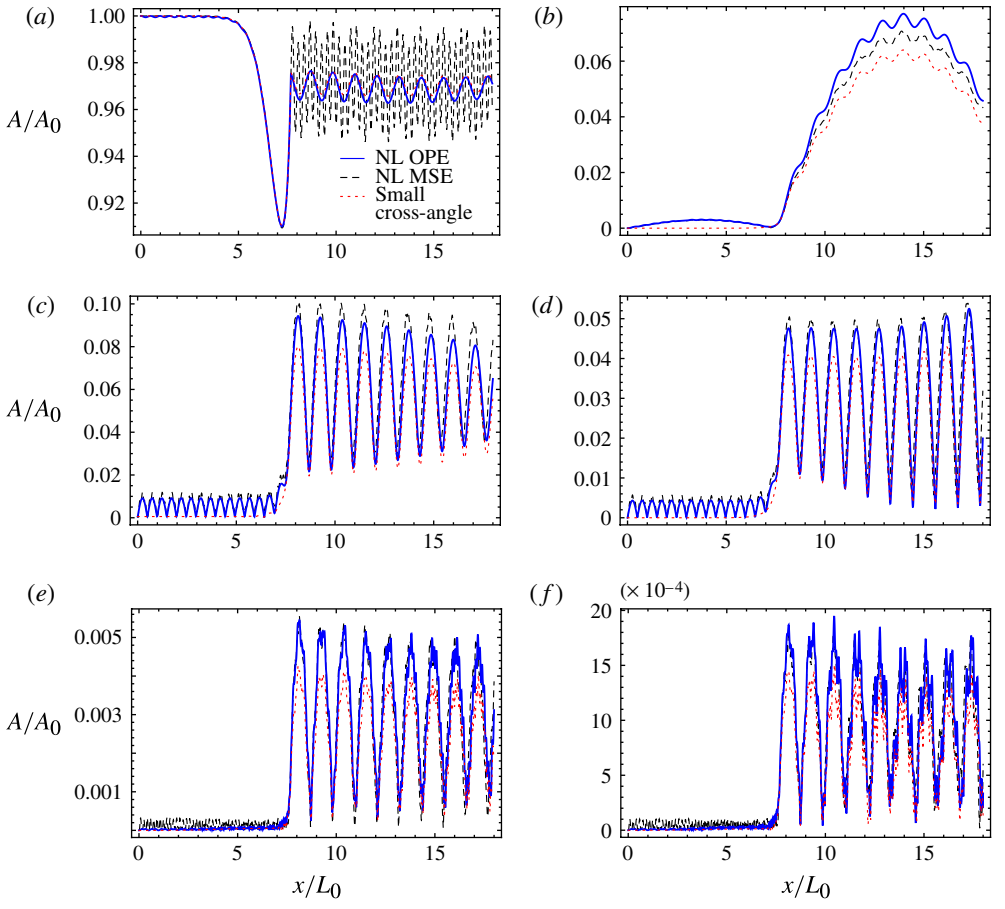


FIGURE 9. (Colour online) The same as figure 7 but for $\theta = \pm 10°$: (*a*) $\phi_{1,1} = \phi_{1,-1}$; (*b*) $\phi_{1,3} = \phi_{1,-3}$; (*c*) $\phi_{2,0}$; (*d*) $\phi_{2,2} = \phi_{2,-2}$; (*e*) $\phi_{3,1} = \phi_{3,-1}$; (*f*) $\phi_{3,3} = \phi_{3,-3}$.

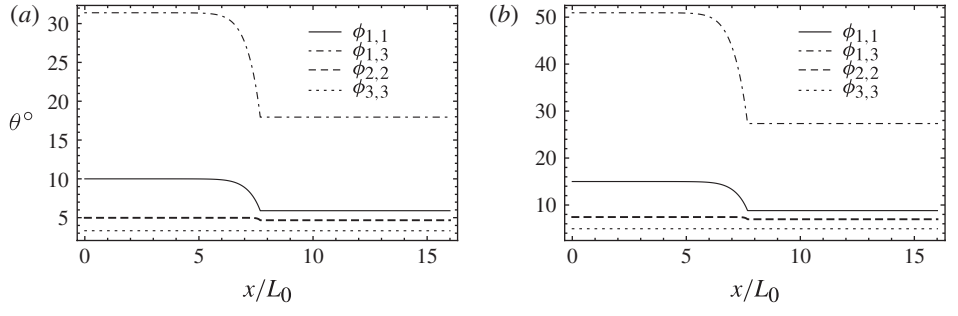


FIGURE 10. The directions of the wave components $\phi_{1,1}$, $\phi_{1,3}$, $\phi_{2,2}$ and $\phi_{3,3}$ (the same for each model) are presented using solid, dot-dashed, dashed and dotted black lines respectively. The two panels relate to the shoaling problems of two waves propagating in initial oblique angles of: (*a*) $\theta_i = \pm 10°$ (corresponding to figure 9); and (*b*) $\theta_i = \pm 15°$ (corresponding to figure 7).

https://doi.org/10.1017/jfm.2012.502 Published online by Cambridge University Press

In the case discussed above the second-harmonic wave was weak since it was generated through the nonlinear interaction. However, in realistic scenarios the wave spectrum consists of various wave harmonics. In the shoaling process, nonlinear sub-harmonic interactions will take place between these waves, transferring a significant amount of energy to larger attack angles. The majority of the wave energy will still reduce its attack angle as in the linear case, but even small amounts of wave energy approaching the beach at larger attack angles may have a significant impact on coastal constructions and their environment. For example, it can agitate harbours and increase long-shore sediment transport.

Acknowledgement

The generous support of the Alexander von Humboldt foundation postdoctoral fellowship is greatly appreciated.

Appendix A. Derivation of the second-order relation between the velocity potential and the surface elevation amplitudes

In § 6 the second-order relationship between the modal and directional base functions of the velocity potential and those of the surface elevations was given. A detailed derivation of this relationship is presented in this appendix.

The second-order nonlinear relation between the surface elevation and the velocity potential was given in (6.3) as

$$\eta = -\frac{1}{g}\frac{\partial \Phi}{\partial t} - \frac{1}{2g}|\nabla \Phi|^2 - \frac{1}{2g}\left(\frac{\partial \Phi}{\partial z}\right)^2 + \frac{1}{g^2}\frac{\partial \Phi}{\partial t}\frac{\partial^2 \Phi}{\partial z \partial t}, \quad z = 0. \tag{A 1}$$

Let us write each nonlinear term of (A 1) in terms of the modal amplitudes of the velocity potential. This is done by applying (2.5), (2.6) and (5.2) to the nonlinear terms of (A 1) as follows:

$$\begin{aligned}
|\nabla \Phi|^2 &= \frac{1}{4}\sum_{l_1=1}^{N}\sum_{m_1=-M}^{M} \nabla\left(\phi_{l_1,m_1} \mathrm{e}^{-\mathrm{i}\omega_{l_1} t} + \phi^*_{l_1,m_1} \mathrm{e}^{\mathrm{i}\omega_{l_1} t}\right) \\
&\quad \times \sum_{l_2=1}^{N}\sum_{m_2=-M}^{M} \nabla\left(\phi_{l_2,m_2} \mathrm{e}^{-\mathrm{i}\omega_{l_2} t} + \phi^*_{l_2,m_2} \mathrm{e}^{\mathrm{i}\omega_{l_2} t}\right) \\
&= -\frac{1}{4}\sum_{l_{1,2}=1}^{N}\sum_{m_{1,2}=-M}^{M} \left(\phi_{l_1,m_1} \mathrm{e}^{-\mathrm{i}\omega_{l_1} t} + \phi^*_{l_1,m_1} \mathrm{e}^{\mathrm{i}\omega_{l_1} t}\right) \\
&\quad \times \left(\phi_{l_2,m_2} \mathrm{e}^{-\mathrm{i}\omega_{l_2} t} + \phi^*_{l_2,m_2} \mathrm{e}^{\mathrm{i}\omega_{l_2} t}\right)\left(k_{1,l_1,m_1} k_{1,l_2,m_2} + k_{2,l_1,m_1} k_{2,l_2,m_2}\right) \\
&= -\frac{1}{4}\sum_{l_{1,2}=1}^{N}\sum_{m_{1,2}=-M}^{M} \Big[\phi_{l_1,m_1}\phi_{l_2,m_2} \mathrm{e}^{-\mathrm{i}\left(\omega_{l_1}+\omega_{l_2}\right)t} \\
&\quad - 2\phi^*_{l_1,m_1}\phi_{l_2,m_2} \mathrm{e}^{-\mathrm{i}\left(\omega_{l_2}-\omega_{l_1}\right)t} - \phi^*_{l_1,m_1}\phi^*_{l_2,m_2} \mathrm{e}^{\mathrm{i}\left(\omega_{l_1}+\omega_{l_2}\right)t}\Big] \\
&\quad \times \left(k_{1,l_1,m_1} k_{1,l_2,m_2} + k_{2,l_1,m_1} k_{2,l_2,m_2}\right),
\end{aligned} \tag{A 2}$$

https://doi.org/10.1017/jfm.2012.502 Published online by Cambridge University Press

$$\left(\frac{\partial \Phi}{\partial z}\right)^2 = \frac{1}{4}\sum_{l_1=1}^{N}\sum_{m_1=-M}^{M}\frac{\omega_{l_1}^2}{g}\left(\phi_{l_1,m_1}\mathrm{e}^{-\mathrm{i}\omega_{l_1}t}+\phi_{l_1,m_1}^{*}\mathrm{e}^{\mathrm{i}\omega_{l_1}t}\right)$$
$$\times\sum_{l_2=1}^{N}\sum_{m_2=-M}^{M}\frac{\omega_{l_2}^2}{g}\left(\phi_{l_2,m_2}\mathrm{e}^{-\mathrm{i}\omega_{l_2}t}+\phi_{l_2,m_2}^{*}\mathrm{e}^{\mathrm{i}\omega_{l_2}t}\right)$$
$$=\frac{1}{4}\sum_{l_{1,2}=1}^{N}\sum_{m_{1,2}=-M}^{M}\left[\phi_{l_1,m_1}\phi_{l_2,m_2}\mathrm{e}^{-\mathrm{i}\left(\omega_{l_1}+\omega_{l_2}\right)t}\right.$$
$$\left.+2\phi_{l_1,m_1}^{*}\phi_{l_2,m_2}\mathrm{e}^{-\mathrm{i}\left(\omega_{l_2}-\omega_{l_1}\right)t}+\phi_{l_1,m_1}^{*}\phi_{l_2,m_2}^{*}\mathrm{e}^{\mathrm{i}\left(\omega_{l_1}+\omega_{l_2}\right)t}\right]\frac{\omega_{l_1}^2\omega_{l_2}^2}{g^2}, \tag{A 3}$$

$$\frac{\partial \Phi}{\partial t}\frac{\partial^2 \Phi}{\partial z\partial t} = \frac{1}{4}\sum_{l_1=1}^{N}\sum_{m_1=-M}^{M}\mathrm{i}\omega_{l_1}\left(-\phi_{l_1,m_1}\mathrm{e}^{-\mathrm{i}\omega_{l_1}t}+\phi_{l_1,m_1}^{*}\mathrm{e}^{\mathrm{i}\omega_{l_1}t}\right)$$
$$\times\sum_{l_2=1}^{N}\sum_{m_2=-M}^{M}\frac{\mathrm{i}\omega_{l_2}^3}{g}\left(-\phi_{l_2,m_2}\mathrm{e}^{-\mathrm{i}\omega_{l_2}t}+\phi_{l_2,m_2}^{*}\mathrm{e}^{\mathrm{i}\omega_{l_2}t}\right)$$
$$=-\frac{1}{4}\sum_{l_{1,2}=1}^{N}\sum_{m_{1,2}=-M}^{M}\left[\frac{\omega_{l_1}\omega_{l_2}^3}{g}\phi_{l_1,m_1}\phi_{l_2,m_2}\mathrm{e}^{-\mathrm{i}\left(\omega_{l_1}+\omega_{l_2}\right)t}\right.$$
$$-\frac{\omega_{l_1}\omega_{l_2}}{g}\left(\omega_{l_1}^2+\omega_{l_2}^2\right)\phi_{l_1,m_1}^{*}\phi_{l_2,m_2}\mathrm{e}^{-\mathrm{i}\left(\omega_{l_2}-\omega_{l_1}\right)t}$$
$$\left.+\frac{\omega_{l_1}\omega_{l_2}^3}{g}\phi_{l_1,m_1}^{*}\phi_{l_2,m_2}^{*}\mathrm{e}^{+\mathrm{i}\left(\omega_{l_1}+\omega_{l_2}\right)t}\right]. \tag{A 4}$$

Equations (A 2)–(A 4) can then be written for the modal component n in the following manner:

$$\left[|\nabla\Phi|^2\right]_n = -\frac{1}{4}\sum_{l=1}^{n-1}\sum_{m_{1,2}=-M}^{M}\left(k_{1,l,m_1}k_{1,n-l,m_2}+k_{2,l,m_1}k_{2,n-l,m_2}\right)\phi_{l,m_1}\phi_{n-l,m_2}$$
$$+\frac{1}{2}\sum_{l=1}^{N-n}\sum_{m_{1,2}=-M}^{M}\left(k_{1,l,m_1}k_{1,n+l,m_2}+k_{2,l,m_1}k_{2,n+l,m_2}\right)\phi_{l,m_1}^{*}\phi_{n+l,m_2}, \tag{A 5}$$

$$\left[\left(\frac{\partial \Phi}{\partial z}\right)^2\right]_n = \frac{1}{4}\sum_{l=1}^{n-1}\sum_{m_{1,2}=-M}^{M}\frac{\omega_l^2\omega_{n-l}^2}{g^2}\phi_{l,m_1}\phi_{n-l,m_2}\mathrm{e}^{\mathrm{i}\left(S_{l,m_1}+S_{n-l,m_2}\right)}$$
$$+\frac{1}{2}\sum_{l=1}^{N-n}\sum_{m_{1,2}=-M}^{M}\frac{\omega_l^2\omega_{n+l}^2}{g^2}\phi_{l,m_1}^{*}\phi_{n+l,m_2}, \tag{A 6}$$

$$\left[\frac{\partial \Phi}{\partial t}\frac{\partial^2 \Phi}{\partial z\partial t}\right]_n = -\frac{1}{4}\sum_{l=1}^{n-1}\sum_{m_{1,2}=-M}^{M}\frac{\omega_l\omega_{n-l}^3}{g}\phi_{l,m_1}\phi_{n-l,m_2}$$
$$+\frac{1}{4}\sum_{l=1}^{N-n}\sum_{m_{1,2}=-M}^{M}\frac{\omega_l\omega_{n+l}}{g}\left(\omega_l^2+\omega_{n+l}^2\right)\phi_{l,m_1}^{*}\phi_{n+l,m_2}. \tag{A 7}$$

https://doi.org/10.1017/jfm.2012.502 Published online by Cambridge University Press

The surface elevation can also be described using a superposition of solutions,

$$\eta = \frac{1}{2}\sum_{n=1}^{N}\sum_{m=-M}^{M}\left[\eta_{n,m}(x,y)\mathrm{e}^{-\mathrm{i}\omega_n t} + \eta^*_{n,m}(x,y)\mathrm{e}^{\mathrm{i}\omega_n t}\right]. \tag{A 8}$$

Applying (2.5), (2.6), (5.2) and (A 8) to the linear part of (A 1), while using (A 5)–(A 7) for its nonlinear part, allows us to construct the relation between the two base functions:

$$\begin{aligned}\frac{1}{2}\sum_{m_0=-M}^{M}\eta_{n,m_0} = \frac{1}{2}\frac{\mathrm{i}\omega_n}{g}\sum_{m_0=-M}^{M}\phi_{n,m_0} + \frac{1}{8g^3}\sum_{l=1}^{n-1}\sum_{m_{1,2}=-M}^{M}T^{+}_{(n,l,m_1,m_2)}\phi_{l,m_1}\phi_{n-l,m_2}\\ -\frac{1}{4g^3}\sum_{l=1}^{N-n}\sum_{m_{1,2}=-M}^{M}T^{-}_{(n,l,m_1,m_2)}\phi^*_{l,m_1}\phi_{n+l,m_2},\end{aligned} \tag{A 9}$$

$$T^{+}_{(n,l,m_1,m_2)} = g^2\left(k_{1,l,m_1}k_{1,n-l,m_2} + k_{2,l,m_1}k_{2,n-l,m_2}\right) - \omega_l^2\omega_{n-l}^2 - 2\omega_l\omega_{n-l}^3, \tag{A 10}$$

$$\begin{aligned}T^{-}_{(n,l,m_1,m_2)} = g^2\left(k_{1,l,m_1}k_{1,n+l,m_2} + k_{2,l,m_1}k_{2,n+l,m_2}\right)\\ +\omega_l^2\omega_{n+l}^2 - \omega_l\omega_{n+l}\left(\omega_l^2+\omega_{n+l}^2\right).\end{aligned} \tag{A 11}$$

Finally, the linear equations can be written separately for each wave mode and wave direction together with nonlinear coupling terms as

$$\begin{aligned}\eta_{n,m_0} = \frac{\mathrm{i}\omega_n}{g}\phi_{n,m_0} + \frac{1}{4g^3}\sum_{l=1}^{n-1}\sum_{m_{1,2}=-M}^{M}T^{+}_{(n,l,m_1,m_2)}\phi_{l,m_1}\phi_{n-l,m_2}\mathscr{D}^{+}_{(n,l,m_0,m_1,m_2)}\\ -\frac{1}{2g^3}\sum_{l=1}^{N-n}\sum_{m_{1,2}=-M}^{M}T^{-}_{(n,l,m_1,m_2)}\phi^*_{l,m_1}\phi_{n+l,m_2}\mathscr{D}^{-}_{(n,l,m_0,m_1,m_2)},\end{aligned} \tag{A 12}$$

$$T^{+}_{(n,l,m_1,m_2)} = g^2\left(k_{1,l,m_1}k_{1,n-l,m_2} + k_{2,l,m_1}k_{2,n-l,m_2}\right) - \omega_l^2\omega_{n-l}^2 - 2\omega_l\omega_{n-l}^3, \tag{A 13}$$

$$\begin{aligned}T^{-}_{(n,l,m_1,m_2)} = g^2\left(k_{1,l,m_1}k_{1,n+l,m_2} + k_{2,l,m_1}k_{2,n+l,m_2}\right)\\ +\omega_l^2\omega_{n+l}^2 - \omega_l\omega_{n+l}\left(\omega_l^2+\omega_{n+l}^2\right),\end{aligned} \tag{A 14}$$

where $\mathscr{D}^{\pm}$ is defined in (5.9).

Appendix B. The improvement avoiding the small crossing angle assumption

The nonlinear part of the elliptic mild-slope model given in (2.9) includes directional terms of the form

$$\nabla\phi_l\cdot\nabla\phi_{n-l}, \quad \nabla\phi^*_l\cdot\nabla\phi_{n+l}. \tag{B 1}$$

These terms consist of a combination of waves propagating in different directions. In order to simplify these terms, previous formulations (see e.g. Kaihatu & Kirby 1995; Janssen *et al.* 2008) neglected terms of $O((ka)^2\,|\partial h/\partial x|, (ka)^2\,|\partial h/\partial y|, (ka)^2\,|\nabla h|^2)$ and assumed a small crossing angle, which resulted in

$$\nabla\phi_l\cdot\nabla\phi_{n-l} = -k_lk_{n-l}\phi_l\phi_{n-l}, \quad \nabla\phi^*_l\cdot\nabla\phi_{n-l} = k_lk_{n+l}\phi^*_l\phi_{n+l}. \tag{B 2}$$

By neglecting terms of $O((ka)^2\,|\partial h/\partial x|, (ka)^2\,|\partial h/\partial y|, (ka)^2\,|\nabla h|^2)$ without any assumption on crossing angles, the terms in (B 1) for an interaction between two

https://doi.org/10.1017/jfm.2012.502 Published online by Cambridge University Press

waves propagating in two arbitrary directions take the form

$$\nabla\phi_l \cdot \nabla\phi_{n-l} = -\boldsymbol{k}_{l,m_1} \cdot \boldsymbol{k}_{n-l,m_2}\phi_l\phi_{n-l}, \quad \nabla\phi_l^* \cdot \nabla\phi_{n-l} = \boldsymbol{k}_{l,m_1} \cdot \boldsymbol{k}_{n+l,m_2}\phi_l^*\phi_{n+l}. \quad \text{(B 3)}$$

This more accurate form was used in the present derivation (see (5.4)–(5.5)).

The difference between (B 2) and (B 3) can be easily calculated using the definition of the dot product,

$$\begin{aligned} \boldsymbol{k}_{l,m_1} \cdot \boldsymbol{k}_{n\pm l,m_2} &= \|\boldsymbol{k}_{l,m_1}\| \|\boldsymbol{k}_{n\pm l,m_2}\| \cos(\Delta\theta) \\ &= k_l k_{n\pm l} \cos(\Delta\theta), \end{aligned} \quad \text{(B 4)}$$

where $\Delta\theta$ represents the crossing angle between the two interacting waves. For very small crossing angles one can assume $\cos(\Delta\theta) \approx 1$ and use (B 2). However, this assumption is frequently inappropriate. Therefore, (B 3) presents an improvement of the nonlinear representation for parabolic-type models. The inaccuracy of the former approach grows as the crossing angle increases. It is given as follows:

$$\boldsymbol{k}_{l,m_1} \cdot \boldsymbol{k}_{n\pm l,m_2}/k_l k_{n\pm l} = \cos(\Delta\theta). \quad \text{(B 5)}$$

This shows that for two waves propagating at ± 15, ± 22.5 and $\pm 30°$, the error of the nonlinear coefficients incorporated in the small crossing angle assumption is of ~ 13, ~ 29 and 50 % respectively.

REFERENCES

AGNON, Y. 1999 Linear and nonlinear refraction and Bragg scattering of water waves. *Phys. Rev.* E **59**, 1319–1322.

AGNON, Y., SHEREMET, A., GONSALVES, J. & STIASSNIE, M. 1993 A unidirectional model for shoaling gravity waves. *Coast. Engng* **20**, 29–58.

BERKHOFF, J. C. W. 1972 Computation of combined refraction–diffraction. In *Proceedings of the 13th International Conference on Coastal Engineering ASCE*, pp. 471–490.

BIESEL, F. 1952 Study of wave propagation in water of gradually varying depth. In *Gravity Waves*, National Bureau of Standards Circular 521, pp. 243–253.

BREDMOSE, H., AGNON, Y., MADSEN, P. A. & SCHÄFFER, H. A. 2005 Wave transformation models with exact second-order transfer. *Eur. J. Mech.* B **24** (6), 659–682.

CHAMBERLAIN, P. G. & PORTER, D. 1995 The modified mild slope equation. *J. Fluid Mech.* **291**, 393–407.

DALRYMPLE, R. A. & KIRBY, J. T. 1988 Models for very wide-angle water waves and wave diffraction. *J. Fluid Mech.* **192**, 33–50.

DALRYMPLE, R. A. & KIRBY, J. T. 1992 Angular spectrum modelling of water waves. *Rev. Aquatic Sci.* **5** (5,6), 382–404.

DINGEMANS, M. W. 1997 *Water Wave Propagations Over Uneven Bottoms*. World Scientific.

ECKART, C. 1952 The propagation of gravity waves from deep to shallow water. *Natl Bur. Stand.* **Circular 521**, 165–173.

ELDEBERKY, Y. & MADSEN, P. A. 1999 Deterministic and stochastic evolution equations for fully dispersive and weakly nonlinear waves. *Coast. Engng* **38**, 1–24.

GREENE, R. R. 1984 The rational approximation to the acoustic wave equation with bottom interaction. *J. Acoust. Soc. Am.* **76** (6), 1764–1773.

HERBERS, T. H. C. & BURTON, M. C. 1997 Nonlinear shoaling of directionally spread waves on a beach. *J. Geophys. Res.* **102**, 21101–21114.

HSU, T. W., LIN, T. Y., WEN, C. C. & OU, S. H. 2006 A complementary mild-slope equation derived using higher-order depth function for waves obliquely propagating on sloping bottom. *Phys. Fluids* **18** (8), 087106.

HSU, T.-W. & WEN, C.-C. 2001 A parabolic equation extended to account for rapidly varying topography. *Ocean Engng* **28** (11), 1479–1498.

https://doi.org/10.1017/jfm.2012.502 Published online by Cambridge University Press

ISOBE, M. 1987 A parabolic equation model for transformation of irregular waves due to reflection, diffraction and breaking. *Coast. Engng Japan* **30** (1), 33–47.

JANSSEN, T. T., HERBERS, T. H. C. & BATTJES, J. A. 2006 Generalized evolution equation for nonlinear surface gravity waves over two-dimensional topography. *J. Fluid Mech.* **552**, 393–418.

JANSSEN, T. T., HERBERS, T. H. C. & BATTJES, J. A. 2008 Evolution of ocean wave statistics in shallow water: refraction and diffraction over seafloor topography. *J. Geophys. Res.* **113**, C03024.

JOHNSON, H. K. & POULIN, S. 2000 On the accuracy of parabolic wave models. In *Proceedings of the 26th International Conference Coastal Engineering, Copenhagen, Denmark*, pp. 352–365.

KAIHATU, J. M. 2001 Improvement of parabolic nonlinear dispersive wave model. *J. Waterways Port Coast. Ocean Engng* **127** (2), 113–121.

KAIHATU, J. M. & KIRBY, J. T. 1995 Nonlinear transformation of waves in finite water depth. *Phys. Fluids* **8**, 175–188.

KIM, J. W. & BAI, K. J. 2004 A new complementary mild-slope equation. *J. Fluid Mech.* **511**, 25–40.

KIRBY, J. T. 1986*a* Higher-order approximations in the parabolic equation method for water waves. *J. Geophys. Res.* **91** (C1), 933–952.

KIRBY, J. T. 1986*b* Rational approximations in the parabolic equation method for water waves. *Coast. Engng* **10** (4), 355–378.

LIU, P.-L. F. & MEI, C. C. 1976 Water motion on a beach in the presence of a breakwater. Part 1. Waves. *J. Geophys. Res.* **81** (18), 3079–3084.

LIU, P. L.-F. & TSAY, T.-K. 1983 On weak reflection of water waves. *J. Fluid Mech.* **131**, 59–71.

LIU, P. L.-F. & TSAY, T.-K. 1985 Numerical prediction of wave transformation. *J. Waterways Port Coast. Ocean Engng* **111** (5), 843–855.

LIU, Y. & YUE, D. K. P. 1998*a* On generalized Bragg scattering of surface waves by bottom ripples. *J. Fluid Mech.* **356**, 297–326.

LIU, Y. & YUE, D. K. P. 1998*b* On generalized Bragg scattering of surface waves by bottom ripples. *J. Fluid Mech.* **356**, 297–326.

LOZANO, C. J. & LIU, P. L. F. 1980 Refraction–diffraction model for linear surface water waves. *J. Fluid Mech.* **101**, 705–720.

MARTIN, P. A., DALRYMPLE, R. A. & KIRBY, J. T. 1997 Gravity waves in water of finite depth. In *Advances in Fluid Mechanics* (ed. J. N. Hunt). *Parabolic Modelling of Water Waves*, vol. 10, chap. 5, pp. 169–213. Computational Mechanics Publications.

MASE, H. 2001 Multidirectional random wave transformation model based on energy balance equation. *Coast. Engng J.* **43** (4), 317–337.

MASSEL, S. R. 1993 Extended refraction–diffraction equation for surface waves. *Coast. Engng* **19**, 97–126.

MCDANIEL, S. T. 1975 Parabolic approximations for underwater sound propagation. *J. Acoust. Soc. Am.* **58** (6), 1178–1185.

PORTER, D. 2003 The mild-slope equations. *J. Fluid Mech.* **494**, 51–63.

PORTER, D. & STAZIKER, D. J. 1995 Extensions of the mild-slope equation. *J. Fluid Mech.* **300**, 367–382.

PORTER, R. & PORTER, D. 2006 Approximations to the scattering of water waves by steep topography. *J. Fluid Mech.* **562**, 279–302.

RADDER, A. C. 1979 On the parabolic equation method for water-wave propagation. *J. Fluid Mech.* **95**, 159–176.

SVENDSEN, I. A. 1967 The wave equation for gravity waves in water of gradually varying depth. *ISVA, Technical University of Denmark, Basic Research Progress Report* 15, pp. 2–7.

TOLEDO, Y. & AGNON, Y. 2009 Nonlinear refraction–diffraction of water waves: the complementary mild-slope equations. *J. Fluid Mech.* **641**, 509–520.

TOLEDO, Y. & AGNON, Y. 2010*a* A scalar form of the complementary mild-slope equation. *J. Fluid Mech.* **656**, 407–416.

TOLEDO, Y. & AGNON, Y. 2010*b* Three-dimensional application of the complementary mild-slope equation. *Coast. Engng* **58** (1).

https://doi.org/10.1017/jfm.2012.502 Published online by Cambridge University Press

TSAY, T.-K., EBERSOLE, B. A. & LIU, P. L.-F. 1989 Numerical modelling of wave propagation using parabolic approximation with a boundary-fitted co-ordinate system. *Intl J. Numer Meth. Engng* **27** (1), 37–55.

TSAY, T.-K. & LIU, P. L.-F. 1982 Numerical solution of water-wave refraction and diffraction problems in the parabolic approximation. *J. Geophys. Res.* **87** (C10), 7932–7940.

YOUNG, I. R. 1999 *Wind Generated Ocean Waves*. Elsevier.

https://doi.org/10.1017/jfm.2012.502 Published online by Cambridge University Press